CrossMark

ORIGINAL ARTICLE

The Spanish National Earthquake Catalogue: Evolution, precision and completeness

Álvaro González (ORCID)

Abstract This paper details the evolution, precision and completeness of the earthquake catalogue compiled by the Spanish National Geographic Institute. Over 100,000 earthquakes are included in this database, occurred in a region embracing Spain, Portugal, Morocco, Andorra and parts of France and Algeria. The catalogue has improved along time, thanks to the development of the seismic network and the upgrades of the routine data acquisition and analysis. The location precision is found to be much better on the Iberian Peninsula than offshore and benefitted especially from the implementation of modern automatic procedures for hypocentral determinations. The different magnitude scales reported in the catalogue, and effects of their changes, are reviewed. In the Iberian Peninsula, Canary Islands and surroundings, detailed successive maps of magnitude of completeness show an overall improvement over the last decades, particularly sudden when the digital broadband network was deployed. Earthquakes are found to be more frequently recorded during nights and weekends, thanks to the lower artificial noise. Despite most blasts have been filtered out of the catalogue, examples of remaining ones are identified by their spatial clustering around mines and quarries, and their timing at the intervals at which blasts are set off (even at night, in contrast to the common assumption that they only occur during daytime). This work highlights the importance of unveiling the spatial and temporal heterogeneities of earthquake catalogues and aims to help future analyses of the seismicity in the region.

1 Introduction

The capabilities for detecting and characterizing earthquakes in any region are limited and evolve throughout time. Consequently, the resulting earthquake catalogue is far from being obtained under controlled, laboratory-like conditions, and is prone to large temporal and spatial heterogeneities. Modifications of the seismological instrumentation, of the earthquake location routines, or of the procedures for calculating magnitudes will leave their mark on the catalogue. It is of utmost importance to decipher and unveil these heterogeneities and limitations, because, if unnoticed or disregarded, they may invalidate the analyses of earthquake data and hamper reaching

Á. González (✉)
Departamento de Ciencias de la Tierra, Universidad de Zaragoza, Campus Plaza San Francisco, 50009 Zaragoza, Spain
e-mail: alvaro.gonzalez@unizar.es

meaningful conclusions (e.g. Muñoz and Udías 1982; Vere-Jones 1992; Kagan 2003).

The Spanish National Earthquake Catalogue is compiled by the *Instituto Geográfico Nacional* (IGN, the agency responsible for earthquake monitoring and warning at a national level in Spain). It can be freely downloaded online (IGN 2016a). Figure 1 shows the epicentres and the spatial extent of the catalogue (26° N to 45° N, 20° W to 6° E). This region embraces mainland Spain, Portugal, Morocco, Andorra, parts of France and Algeria, and several Portuguese and Spanish archipelagos (Balearic, Canary and Madeira). The catalogue contains data of over 100,000 events, originated since 880 B.C. until present, most of them in recent decades, with a yearly record of $\sim 17{,}000$ in 2011.

At one extreme, this region has experienced the greatest earthquakes in western Europe. The largest known events are the Lisbon Earthquake on 1 November 1755 (moment magnitude $M_w \simeq 8.5$; Martínez Solares and Mezcua 2002; Martínez Solares and Loípez Arroyo 2004), the 25 November 1941 North Atlantic Earthquake ($M_w \simeq 8.0$; Storchak et al. 2013), the 28 February 1969 offshore Portugal earthquake ($M_w = 7.8$; Storchak et al. 2013) and the enigmatic, deep earthquake of Granada (south Spain) on 31 March 1954 ($M_w = 7.8$; Storchak et al. 2013). At the other extreme, earthquakes with magnitudes ≤ 1 are currently reported in the IGN catalogue in the geographic areas with the densest distribution of stations.

The Spanish National Seismic Network (the largest permanent network in the country, managed by IGN) provides the primary data source for the real-time compilation of the catalogue. This is expanded by IGN with data shared by seismic stations of other institutions in Spain and abroad, either in real time, or for the final catalogue review. These additional stations belong, for example, to the regional, permanent Spanish networks in Andalusia (IAG 2016) and Catalonia (ICGC 2016), those of the San Fernando and Ebro observatories, and the national seismic networks of France, Portugal, Morocco and Algeria. More information on permanent networks on the Iberian region can be found in Alguacil and Martín Dávila (2003).

Conversely, this catalogue has been used as a source for others. For example, for Portugal (Carrilho et al. 2004; Pena et al. 2014), Pyrenees (Souriau and Pauchet 1998; Secanell et al. 2008), Catalonia (Susagna and Goula 1999), Algeria and Morocco (e.g. Peláez et al. 2007; Hamdache et al. 2010; Ayadi and Bezzeghoud 2015; Harbi et al. 2015), Euro-Mediterranean region (Grünthal and Wahlström 2012), and the Bulletin of the International Seismological Centre (ISC 2016b). IGN is a nodal centre of the Euro-Mediterranean Seismological Centre

Fig. 1 Epicentres in the Spanish National Earthquake Catalogue since the historical era to the end of 2013, separated according to hypocentral depth. Map in a sinusoidal (equal area) projection, over the global relief model of Amante and Eakins (2009), replaced by the bathymetry of Zitellini et al. (2009) where available. The infrequent earthquakes with depth > 30 km are highlighted by being plotted on top of the others. Depth is considered unknown if absent (e.g. for events located from intensity data only) or fixed (not calculated as an independent parameter)
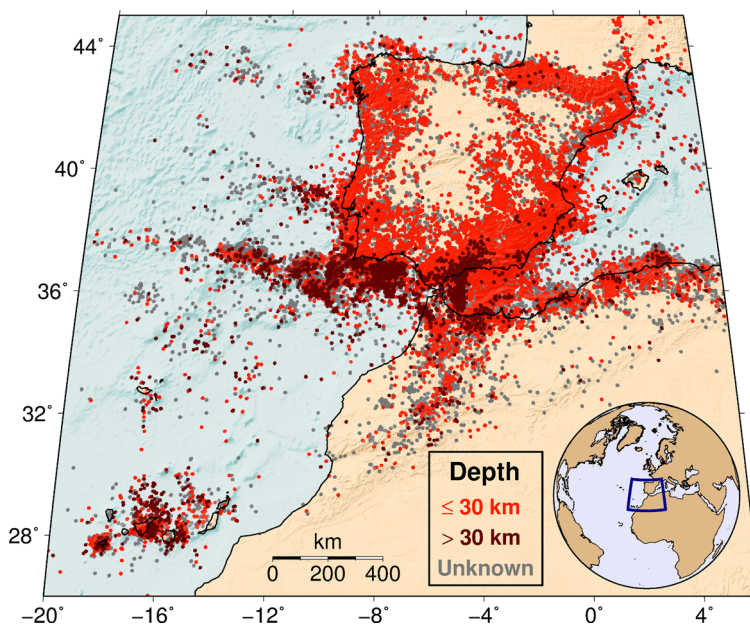
and contributes data for its bulletin (Godey et al. 2006). So analysing the IGN catalogue may eventually contribute to characterizing these separate, but intertwined, databases.

This paper aims to review the evolution of the catalogue and the seismic network, assess the typical precision of hypocentral locations, identify the heterogeneities arising from the different magnitude scales reported, map in detail the magnitude of completeness, evaluate apparent daily and weekly variations of earthquake frequencies and review and exemplify the contamination of the catalogue by quarry and mine blasts. It uses the catalogue data until the end of 2013 ($\sim 98,000$ events in total), the last year for which it has been completely revised.

2 Evolution of the catalogue

Focusing on the main data source, the current catalogue can be divided into three blocks:

– Before 1901, it is mostly based (with later updates) on the catalogue by Martínez Solares and Mezcua (2002) for the Iberian Peninsula and surroundings, and on the earlier one by Mezcua and Martínez Solares (1983) for the Canary Islands.
– From 1901 to 1980, it is taken from Mezcua and Martínez Solares (1983), with later revisions.
– Since 1981, it has been directly compiled by IGN using data provided by the Spanish National Seismic Network (*Red Sísmica Nacional*), and seismological stations of other institutions.

The cumulative number of earthquakes in the catalogue (Fig. 2) shows an apparent increase of the earthquake rate with time (especially for magnitudes ≤ 3), which evidences a progressive improvement of detection capabilities. In the Canary Islands since mid-2011 the increase is mostly natural, due to the surge of volcanic swarms in El Hierro island.

The following subsections review the development of the catalogue and of its data sources, including network instrumentation.

2.1 Historical era (until 1900)

The most damaging earthquakes in Spain occurred in the historical era, until the late nineteenth century, for which the catalogue is based on chronicles that
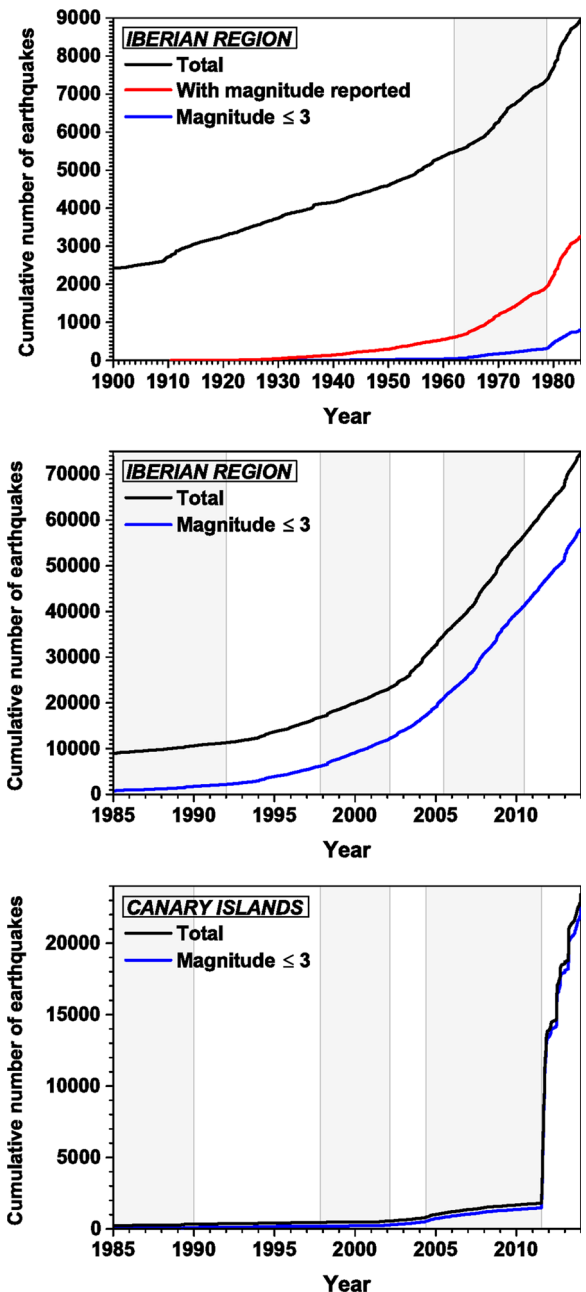

Fig. 2 Cumulative number of earthquakes versus time, in the geographic regions analysed (maps of Figs. 12 and 14). Magnitude is not reported for earthquakes occurred before 1910, while it is reported for the vast majority since 1985 (not shown separately). *Vertical fringes* indicate the periods considered for completeness assessment

describe the effects of the earthquakes. This historical catalogue relies on primary documental sources and on earlier compilations, as discussed by Muñoz

and Udías (1982), Roca et al. (2004), Rodríguez de la Torre (2004) and Udías (2015). The first catalogue entry dates from 880 B.C., although the first Iberian earthquake for which the exact date is known took place on 21 May 881 (Udías 2015). The first event for which the catalogue details both the location and maximum intensity dates from 1048.

A digital database of macroseismic information for earthquakes until 1900 (Roca et al. 2011) is available on the IGN webpage (IGN 2016a). Historic and early instrumental earthquakes in Spain and surroundings are being continually subject to revisions (e.g. Samardjieva et al. 1999; Mezcua et al. 2004, 2013; Udías 2015, and references therein). The first systematic catalogue compiling the geological and archeological effects of earthquakes in Spain has been published by Silva et al. (2014).

2.2 First observatories (1897–1924)

Instrumental recording in Spain and Portugal began in the late nineteenth century, although macroseismic observations would remain the chief data source for the catalogue until the beginning of the strictly instrumental era (Section 2.6). A catalogue of the early Spanish seismographs was compiled by Batlló and Bormann (2000) and Batlló (2004). The first instrumental observations in peninsular Spain were made in 1885 (Martínez Solares 1981; Batlló 2004; Udías 2013) and in the Canary Islands in 1890 (Batlló 2004; Fréchet and Rivera 2012). In Portugal, the first station was installed in Coimbra; it began experimental recording in 1891 and continuous recording in 1903 (Custódio et al. 2012). The first continuous recordings in Spain were made with two Milne seismographs, one installed in 1897 in the Observatory of San Fernando (of the Spanish Royal Navy; Martín Dávila et al. 2006) and the next one in 1898 in the mines of Río Tinto (Udías 2013).

The next two Spanish observatories were founded by the Jesuits (Cartuja, in 1902 and Ebro, in 1904; Udías and Stauder 1996; Anduaga 2004; Ammon et al. 2010) and were followed in 1906 by the Fabra Observatory of the *Academia de Ciencias y Artes de Barcelona*.

The first seismic observatory of the *Instituto Geográfico* (former name of the IGN) was set up in Toledo, near Madrid, in 1909 (Anduaga 2004; Udías 2013). It was crucial for recording early instrumental

earthquakes in the Iberian region, because of its relatively advanced and well maintained instrumentation (e.g. Samardjieva et al. 1997, 1998; Payo Subiza and Gómez-Menor 1998; Badal et al. 2000; Batlló 2004). Next, this Institute opened new observatories in Almería (1911), Málaga (1913) and Alicante (1914) and undertook major upgrades of the seismographic instrumentation used (circa 1924, Anduaga 2004, 2009). It has also been gathering macroseismic data since 1909 (Roca et al. 2004), with detailed questionnaires at least since the 1920s (Servicio Sismológico 1923; Anduaga 2009).

2.3 Printed bulletins (1924–1995)

Parallel to the instrumentation updates, phase picks of instrumentally recorded earthquakes started being reported by the *Instituto Geográfico* in printed bulletins in August 1924. These bulletins have been a primary source of information for the catalogue. Most of them are currently scanned and available online, with gaps for the period of the Spanish Civil War (1936–1939) and 1940s (IGN 2016a; Michelini et al. 2005; Euroseismos Project 2006). The last bulletin reported the seismicity of 1995. Earthquakes occurred since 1996 are only reported in the digital catalogue (see Section 2.14). The bulletin for 1987 was the first to include the seismicity of the Canary Islands.

2.4 Civil War (1936–1939) and postwar

Science in general, and seismology in particular, suffered from the havoc of the Spanish Civil War (1936–1939). During war time, several observatories had to be either abandoned or operated under precarious conditions (Anduaga 2009) resulting in a fragmentary record, evidenced by a decrease of the apparent rate of earthquakes during that period (Rodríguez de la Torre 1989). The effects of the war on observational seismology were long-lasting (Anduaga 2009), and it was not until 1952 (Batlló 2004; ISC 2016a) that the next national seismological station was opened (the first permanent station in the Canary Islands, in Tenerife).

2.5 Systematic earthquake location (1955–present)

Instrumental locations for earthquakes of the first half of the twentieth century were compiled from different databases and not recalculated using a common

procedure (Mezcua and Martínez Solares 1983). The locations of later earthquakes have been systematically computed using software (Section 3): retrospectively by Mezcua and Martínez Solares (1983) for events between 1955 and 1980, and routinely for earthquakes since 1981 (Section 2.14).

2.6 Instrumental era (1962–present)

During the current, instrumental era, seismograms are the main source of information of the IGN catalogue, macroseismic information being complementary.

In the Iberian Peninsula, the onset of this era was marked by the set up of three stations of the World-Wide Standardized Seismographic Network (WWSSN): Toledo and Málaga (Spain) in 1962 and Porto (Portugal) in 1963 (Alguacil and Martín Dávila 2003; López and Muñoz 2003; Martínez Solares 2003; Peterson and Hutt 2014). And a new Spanish national observatory (Logroño) started experimental recording ca. 1961 and full operation in 1963. The last national observatory opened in Santiago, northwestern Iberian Peninsula, in 1972. Since 1962, magnitude is systematically reported for most earthquakes, and an increase in the apparent seismicity rate is noticeable (Fig. 2, top).

In the Canary Islands, the instrumental era is considered to have begun in 1975, when earthquakes in the catalogue became typically characterized by magnitude, instead of by maximum felt intensity (Martínez Solares et al. 2013). This improvement was possible by the opening of two new stations, in the islands of El Hierro and La Palma (in September 1973 and November 1974, respectively, ISC 2016a), together with the station already existing in Tenerife.

2.7 First telemetred network (1978–1992)

The first telemetred seismograph of IGN (located in Sierra de Guadarrama, near Madrid) provided its first phase picks to the catalogue in October 1978. By 1985, up to eight homogenous, short-period, vertical-component IGN stations with common time synchronization and real-time data transmission via telephone lines had been opened in peninsular Spain (e.g. García Fernández et al. 1987), marking the beginning of the *Red Sísmica Nacional Española* (Spanish National Seismic Network, IGN 1991; Carreño et al. 2003; Carreño Herrero and Valero Zornoza 2011). Since

1985, thanks to these enhanced detection capabilities, most earthquakes in the catalogue have magnitude ≤ 3 (Fig. 2).

Two subnetworks have been traditionally considered (e.g. Mezcua 1995): one in the Iberian Peninsula, Balearic Islands and Spanish enclaves in northernmost Africa, and another in the Canary Islands. The stations in the Iberian Peninsula were not regularly spaced, but preferentially located in the onshore areas with the highest seismicity (Mezcua 1995), where also most of the currently known active faults are located (García-Mayordomo et al. 2012).

Figure 3 shows the number of permanent stations of the Spanish National Seismic Network in the Iberian Peninsula and surroundings (mapped in Fig. 4) and the Canary Islands (mapped in Fig. 14). To find out the actual operating period of each station, I took into account the dates at which it reported its first and last phase pick included in the catalogue. Also, if the station was upgraded from short-period to broadband instrumentation (as reported in the station details, IGN 2016a), I considered the first and last picks for each kind of instrumentation. For simplicity, other temporary interruptions were not included in this plot. For most stations, these dates are consistent with the official dates of station openings and closings (IGN 2016a), though there are a few exceptions. Some stations started reporting phase picks before its official opening (probably because they were already installed as temporary stations). Also, a few stations reported phase picks, occasionally, after their official closure. The station data used are provided in the Online Resource 1.

In the Canary Islands, the network was very sparse in the late 1980s (Figs. 3 and 14) and recorded only minor seismicity in these initial years (Mezcua et al. 1992). The need for improved monitoring was already recognized (García Fernández et al. 1988), and highlighted by the occurrence of an earthquake with magnitude 5.2 on May 1989 between the islands of Tenerife and Gran Canaria (Mezcua et al. 1992; Jiménez and García-Fernández 1996; Vinciguerra and Day 2013). This seismic crises prompted the installation of two new permanent stations which started operating in 1990.

The telemetred short-period network was a major improvement with respect to the early observatories, but also had several limitations. The selection of sites for its stations was constrained by the availability
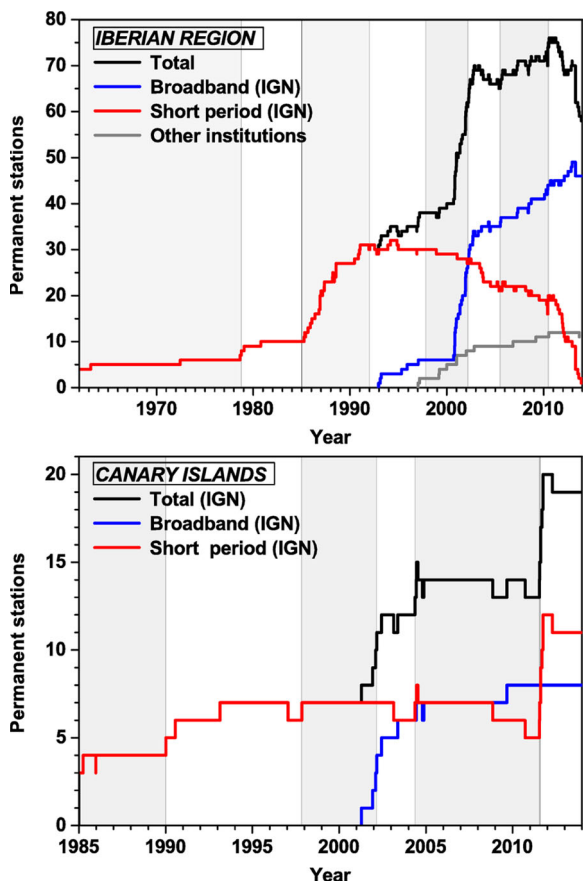
Fig. 3 Number of permanent seismic stations of the National Seismic Network on the Iberian Peninsula and surroundings (*Iberian Region*, for short) *(top)* and on the Canary Islands *(bottom)* reporting phase picks to the catalogue. It is indicated whether the stations are managed by IGN. Stations from other institutions are only included in this plot if they were used for the real-time automatic location procedures. Many other stations from other institutions have been used for elaborating the final catalogue. Station maps are plotted in Figs. 4 and 14, and station data are provided in the Online Resource 1

of communication facilities (García Fernández et al. 1987). Eventually, as urban areas expanded, this implied that most stations suffered from high seismic noise (Canas Torres and Vidal Sánchez 2001). Also, the records of moderate and major earthquakes were frequently saturated and clipped (e.g. Rueda 1995), because of the narrow dynamic range of the telephone lines used for data transmission (Mezcua 1995). This kind of problem (which also affected other networks with similar telemetric systems at the time, e.g. Amato and Mele 2008) is particularly annoying

for calculating reliable magnitudes, since it especially affects the stations closest to the earthquake, which are expected to record it with the highest signal-to-noise ratios (e.g. Yang and Ben-Zion 2010). These issues were not solved until the new digital network was set up (Section 2.11).

2.8 First automatic locations (1991–1997)

In the early 1990s, when the short-period telemetred network reached its maximum development (Figs. 3 and 4), the first automatic procedure for near real-time hypocentral determination was used, which potentially enabled a more systematic and complete detection. It began experimental operation in the spring of 1991 (according to the seismic bulletin for that year) and was detailed by Mezcua (1995) and Rueda (1995). This system was replaced by a more advanced one in late 1997 (Section 2.10).

2.9 The Sonseca Array (1992–present)

The Sonseca Array is a small-aperture array of short-period, long-period and broadband stations, deployed inside boreholes around the town of Sonseca, at the centre of the Iberian Peninsula (IGN 1991; Martínez Solares 1992; Mezcua and Rueda 1994; Mezcua 1995; Dowla 1996; Carreño et al. 2001; Bahavar and North 2002; Hasting and Barrientos 2002; Rueda Núñez 2006; Kværna and Ringdal 2013). Its main purpose has been nuclear explosion monitoring and is currently a primary station of the International Monitoring System of the Comprehensive Nuclear-Test-Ban Treaty Organization. Opened in February 1957, it was initially owned by the United States of America, until 1996, when it was formally transferred to the IGN. Data from this array had already started being received by IGN in 1988 (Mezcua 1995) and in real time from mid-1989 (IGN 2016a). It became fully integrated into the permanent IGN network in 1992 (Rueda Núñez 2006) and provided the first phase pick to the catalogue in December of that year. The Sonseca Array has been upgraded several times (Hasting and Barrientos 2002), and its long-period instruments, located on the outer part of the array, were removed in June 2010 (Fig. 4).

The Sonseca Array usually contributes to the hypocentral determination as a single station with superior signal detection capability (Sonseca Array
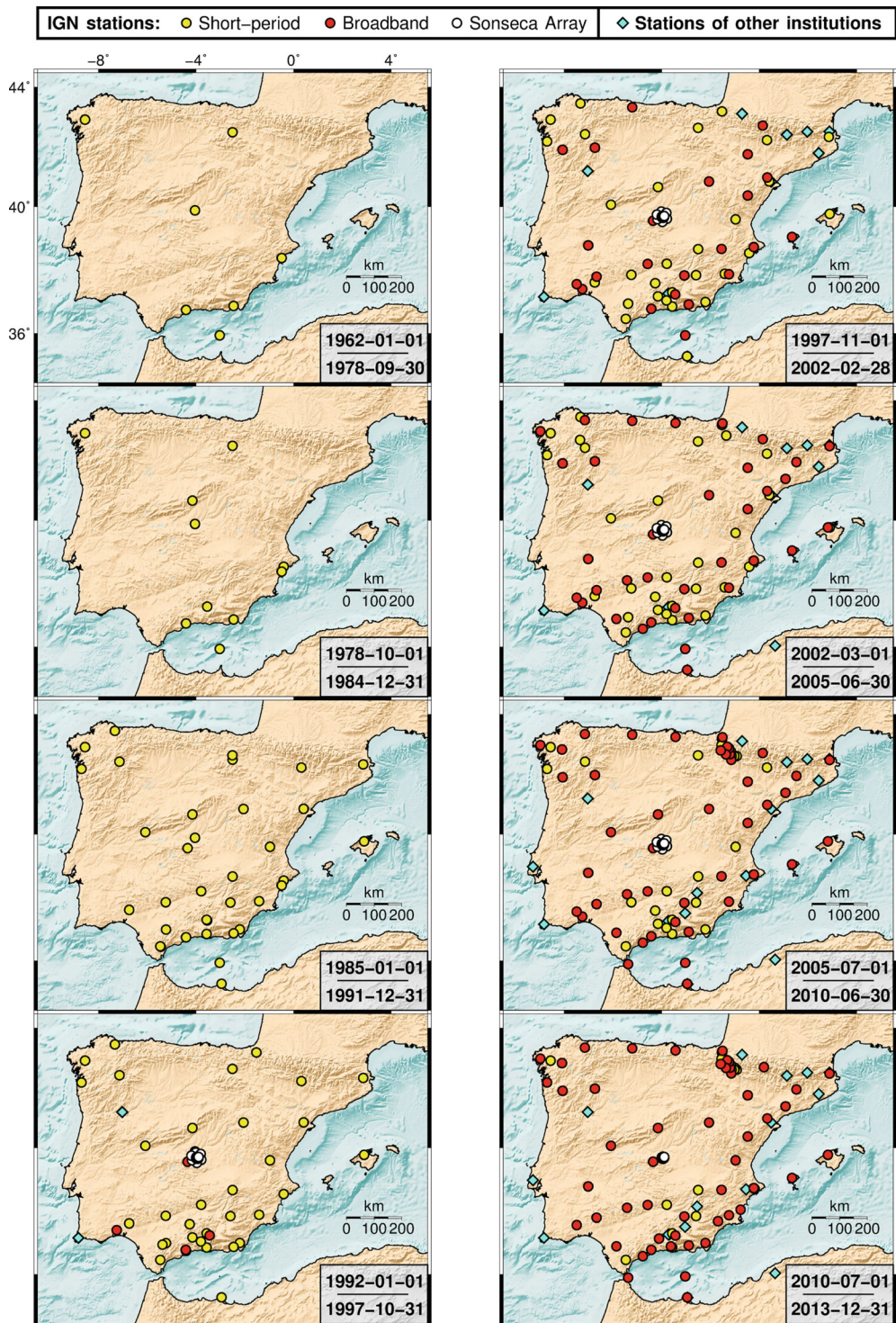
Fig. 4 Seismic stations in the Iberian Peninsula and surroundings, for the periods considered for completeness assessment (Fig. 12). They are either owned by the Instituto Geográfico Nacional (*circles*), or by other institutions (*squares*) but whose data have been used for real-time hypocentral determinations by IGN. Data from other stations (not shown) have been used to elaborate the final, revised catalogue. Each map includes the stations for which the catalogue reports phase picks during at least part of the corresponding period. Station data are provided in the Online Resource 1

beam reference point, station code ESDC, ISC 2016a). To do so, the records of the array elements are combined into a single one, using beam-forming techniques which enhance the signal-to-noise ratio and provide the velocity vector of an incoming wavefront (its back azimuth and slowness, e.g. Rost and Thomas 2002; Rueda Núñez 2006; Schweitzer et al. 2009). This makes such array particularly valuable for locating events (e.g. Martínez Solares 1992, 1995; Rueda 1995). The array instruments typically do not supply phase picks individually to the catalogue, since this would imply an excessive number of observations recorded at almost exactly the same azimuth, that could cause a hypocentral location bias (Rueda 1995). The main exception is the broadband station with code ESLA (ISC 2016a), included in the array, which did contribute numerous picks individually, and is included separately in Fig. 3.

Because of its sensitivity, and despite ESDC being located somewhat far from seismically active areas, it provides more data to the catalogue than other stations; in particular, it is the one which until 2013 contributed more phase picks for earthquakes with $M \geq 2.0$ in the Iberian Peninsula and its close surroundings (36° N–44° N, 10° W–4° E).

2.10 New automatic earthquake location and stations from other institutions (1997–present)

In November 1997, complex automatic location procedures came into use (Carreño et al. 2003), using the EvLoc location software (Nagy 1996). Since then, this software has been used to calculate the final locations in the catalogue (Carreño Herrero and Valero Zornoza 2011) and will be discussed in more detail in Section 3.

From 1997 onwards, stations from other institutions are used for the automatic real-time hypocentral defterminations, so they are in practice an extension of the Spanish National Seismic Network (Figs. 3 and 4). The whole set of permanent stations involved in real-time earthquake location will be referred to here as the *backbone network*. For elaborating the final catalogue, IGN uses data from additional stations, eventually provided (not in real time) by other institutions (Section 2.14).

2.11 Broadband network (1999–present)

The first few broadband stations of the Spanish National Seismic Network were installed in the 1990s (Fig. 3 and Mezcua 1995). In the late 1999, installation commenced on the new network of three-component, digital broadband stations (*Red Sísmica Digital Española*, Spanish Digital Seismic Network). Data are transmitted via satellite for most of them, so they could be sited even in remote locations with low seismic noise.

The fast initial deployment of the first set of new stations was completed in 2002; since then, the number of broadband IGN stations has increased more slowly (Fig. 3). Thanks to the broadband network, the number of located events per unit time increased significantly from 2002 onwards (Fig. 2 and Carreño et al. 2003), especially for those with $M \leq 3$ (but see Section 4.6 for the effect of magnitude changes). Concomitantly to the deployment of broadband stations, the analog short-period stations have been progressively replaced or closed down, especially in the Iberian Peninsula (Fig. 3). Rueda and Mezcua (2015) have presented a recent overview of this broadband network and analysed the instrument orientations.

2.12 Monitoring around the Itoiz and Yesa reservoirs (2005–2013)

Apart from the Sonseca Array, the Aragón River Valley, in the Western Pyrenees, eventually became the geographic region where the IGN network was densest in the Iberian Peninsula (Fig. 4). Fourteen three-component stations (3 broadband and 11 short-period) and an accelerometric network were progressively deployed there between mid-2005 and mid-2010 (apart from two broadband stations already existing). Their purpose was to monitor in great detail the seismicity in the surroundings of two large water reservoirs, Itoiz and Yesa. This was motivated by a $M_w = 4.5$ earthquake on 18 September 2004, possibly triggered by the first impoundment of the recently-built Itoiz reservoir (Ruiz et al. 2006; Durá-Gómez and Talwani 2010; Luzón et al. 2010; Santoyo et al. 2010). Most of these stations were closed down between mid-2011 and late-2013, leaving the Spanish

National Seismic Network in the Iberian Peninsula almost devoid of short-period stations by the end of 2013 (Fig. 3).

2.13 Monitoring of seismo-volcanic activity in the Canary Islands (2004 and 2011–present)

In the Canary Islands, two network improvements were spurred by seismic crises which started in 2004 and 2011.

In Tenerife, a seismic swarm took place in 2004, starting in April (e.g. Almendros et al. 2007; Martí et al. 2009; Domínguez Cerdeña et al. 2011 and references therein). Three additional permanent seismic stations (two short-period and one broadband) were installed on the island between May–June 2004 (the first one in 17 May), plus two temporary ones which operated intermittently from June to November 2014 (not considered in Fig. 3, Domínguez Cerdeña 2011). This episode noticeably increased the recorded earthquake rate (Fig. 2). The short-period stations stopped contributing to the catalogue in 2008 and 2010, respectively.

Increased activity on 19 July 2011 on El Hierro (the southwesternmost island) led to dedicated geophysical monitoring, including up to nine new short-period seismic stations, most of them three-component (López et al. 2012; Domínguez Cerdeña et al. 2014). Seven of these stations have contributed data to the IGN catalogue (Fig. 3), the first one starting on 21 July. The seismic activity continued for months (Ibáñez et al. 2012; Domínguez Cerdeña et al. 2014), preceding a submarine eruption which started on 10 October 2011 off the southern shore of the island, and which was declared finished as of 5 March 2012. Several seismic swarms ensued, related to magma intrusions (the first ones described by García et al. 2014, and later ones until 2014). Until the end of 2013, this activity on El Hierro added ∼ 20, 000 earthquakes to the catalogue (Fig. 2).

2.14 Current practice on catalogue compilation

For each detected event, a preliminary, automatic determination of hypocentral location and magnitude is calculated automatically in real time and posted online. These initial determinations are then updated after a manual review by the around-the-clock Seismic Information Service of IGN (IGN 2016a).

The catalogue data may be eventually subjected to further reviews. It can be regarded as fully revised only after being updated in yearly blocks, with an irregular delay of about 18–24 months (similarly as the former annual printed bulletins). As with other catalogues (e.g. Willemam and Storchak 2001), this long latency period allows for a careful data review and incorporation of phase pick information eventually delivered by other collaborating institutions (e.g. in Spain, Portugal, France, Morocco, and Algeria). This additional data improves the catalogue especially for large earthquakes (which can potentially be detected at larger distances by other stations), or in general for earthquakes occurring where networks from other institutions have better coverage. That is, the revised catalogue is more complete than the detection threshold of the Spanish National Seismic Network alone would allow (e.g. García Fernández 1986). Occasionally, specific earthquakes are subject to later reviews if new information or improved analyses are available. At the time of this writing, the catalogue is reviewed up to the end of 2013.

From the IGN webpage, the catalogue may be downloaded in two versions. The abridged version (option labelled as "without phase readings") provides a list of data about origin time, location, preferred magnitude and maximum intensity, for earthquakes from the historical period to present. The full version (option "with phase readings") is available online only for earthquakes since November 1997 until the present and provides a catalogue in the IMS1.0 standard format (Biegalski et al. 1999), which includes the uncertainties of origin time, location and magnitude, and the list of phase picks from all the stations used to locate the event and calculate its magnitude. It also specifies the date at which the data for each earthquake were generated (i.e. the date of the last review), and the "author" field is reported as "`IGN`" for the preliminary solutions and as "`bull_2`" for the final ones. The full version of the digital catalogue for earthquakes between January 1983 and October 1997 (used in Section 3) has other formats and is available by request to IGN (see contact information for seismology on their web page). Moment tensor and moment magnitude calculations (Rueda and Mezcua

2005) are provided in a separate database online (IGN 2016a).

The Spanish Accelerograph Network (managed by IGN) started being deployed in 1974 and was described by Carreño et al. (1991b), Mezcua (1995) and Mezcua et al. (2008). Accelerograms with timing calibrated by GPS are occasionally used to improve the hypocentral determinations in the IGN catalogue, e.g. for the earthquakes of Lorca (southeastern Iberian Peninsula) in 2011 (Cabañas et al. 2014; Morales et al. 2014), the latest damaging ones in Spain (Martínez-Díaz et al. 2012). At least since the 1970s, IGN also deploys temporary networks for microseismicity surveys or aftershock monitoring (e.g. seismic bulletin for 1977, Carreño et al. 1991a; Herraiz and Lázaro 1991).

Macroseismic information is compiled by IGN using questionnaires, and in real time by means of felt reports contributed online by witnesses (IGN 2016a).

3 Precision of earthquake locations

For most earthquakes, the catalogue specifies the precision of the hypocentral location (the formal uncertainty due to random errors, e.g. Husen and Hardebeck 2010). The actual accuracy of a location may be worse, because of additional, systematic errors (e.g. in the velocity model used, Havskov and Ottemöller 2010; Husen and Hardebeck 2010); it can be assessed only if the exact location is known independently (such as in a controlled explosion source, e.g. Yang et al. 2004; Havskov and Ottemöller 2010).

The typical uncertainty of hypocentral locations varies in time (due to changes in the network and in location procedures) and in space. Events occurring far from the network are expected to have the largest uncertainties (e.g. García Fernández 1986, 1987; Rueda Núñez 2006; D'Alessandro et al. 2013; Cesca et al. 2013; Custódio et al. 2015), because they are typically recorded by few stations and with a large azimuthal gap (the largest angular gap in azimuth from the epicentre to azimuthally adjacent stations, e.g. Havskov and Ottemöller 2010).

3.1 Location procedures

Instrumental locations in the IGN catalogue are single-event (i.e. calculated for each earthquake individually, based on the picks of wave phase arrivals at each station), using layered, 1-D velocity models. In the Iberian Peninsula and surroundings, the model used by Mezcua and Martínez Solares (1983) for earthquakes occurred since 1955 has been adopted for routine locations by IGN until today (IGN bulletins, Carreño et al. 2003; Carreño Herrero and Valero Zornoza 2011). For moment-tensor determinations by IGN, the model for the Iberian Peninsula and surroundings has an additional, shallow layer with lower seismic velocities (Rueda and Mezcua 2005). In the Canary Islands and surroundings (19° W–13° W, 27° N–30° N) a different model (labelled as "Canary") is being used; it was specified for the first time in the Bulletin for 1987 (the first one reporting earthquakes from this archipelago) and, according to Rueda Núñez (2006), is an average of the models proposed by Dañobeitia (1980) for each island. From January 2004 to December 2014, a different model (labelled as "Teide") has been used for locating earthquakes under the Teide stratovolcano (Tenerife Island). It is actually a model for the Etna volcano (Scarpa et al. 1983), which had been shown able to improve earthquake locations also in the Teide (Almendros et al. 2000), with the Moho discontinuity depth adapted to match that of the Canary model. Both P and S waves are used for calculating the revised hypocentral locations since 1955 (e.g. Rueda 1995), with a fixed velocity ratio $V_P/V_S = 1.75$ (IGN bulletin for 1987, Rueda 1995; Carreño et al. 2003; Rueda and Mezcua 2006). D'Alessandro et al. (2013) discussed the limitations of the velocity model used by IGN for the Iberian region, although they assumed a different ratio ($V_P/V_S = 1.73$) and that the same model was also used for the Canary Islands. The full-format catalogue specifies the model used for locating each earthquake (if different from the default one of the Iberian region).

Double-difference relocations (Waldhauser and Ellsworth 2000) have been calculated by IGN and collaborators in specific case studies, such as for the 2011 Lorca earthquake series (Morales et al. 2014),

and for the seismo-volcanic swarms of 2004–2005 in Tenerife (Domínguez Cerdeña et al. 2011) and of 2011 in El Hierro (Domínguez Cerdeña et al. 2014). The relocated catalogues for the Canary Islands can be downloaded separately from the IGN webpage (IGN 2016b).

Before the strictly instrumental era, location uncertainties may be substantial, given that the early mechanical seismometers (Batlló 2004) lacked common timing. For example, the catalogue locations of an earthquake sequence in southern Spain in 1951 are now taken from Batlló (2008, see also references therein) and corrected the earlier ones (taken from Mezcua and Martínez Solares 1983) by tens of kilometres. No location uncertainties are reported in the catalogue for the first half of the twentieth century.

For earthquakes since 1955 until October 1997, Hypo71 (Lee and Lahr 1975) was used to calculate the final, revised hypocentral locations (IGN Bulletins, Mezcua and Martínez Solares 1983; Carreño et al. 2003). The only source of uncertainty that this software accounts for is the measurement error inherent to each arrival time, assumed random and normally (Gaussian) distributed (e.g. Boyd and Snoke 1984). The location uncertainties calculated with Hypo71 were reported by Mezcua and Martínez Solares (1983) for a few events in the 1950s and for the majority of earthquakes from 1960 to 1980. From 1981 to 1995, they are reported in most IGN bulletins.

The digital full-format catalogue from January 1983 to October 1997 (Resurrección Antón, IGN, pers. comm., 2012; not available online) will be used here for analysing location precision in this first period. In 1983–1984, an average of $\sim$ 11 phases were used for each earthquake location, which rose to $\sim$ 20 from January 1985 to October 1997. Hypo71 handles a default maximum of 100 phases for each earthquake (Lee and Lahr 1975), and indeed before November 1997, only three earthquakes were located with a higher figure.

Since November 1997, hypocentral locations and their uncertainties are reported in the full-format catalogue online (IGN 2016a), and have been calculated with Evloc (Carreño Herrero and Valero Zornoza 2011 and Resurrección Antón, IGN, pers. comm., 2015). This software (Nagy 1996) implements the method by Bratt and Bache (1988) and allows taking into account random errors not only in measurements (phase pickings) but also those resulting from modelling (e.g. Yang et al. 2004). The number of phases used for locating each earthquake with Evloc has been highly variable, with an average of $\sim$ 24, with $\geq$ 30 or more phases in 22 % of events, and $\geq$ 100 phases for 2 % of events.

3.2 Epicentral location

Before November 1997, epicentral location uncertainties were calculated with Hypo71 and specified as the so-called ERH (standard horizontal error, in km). Unfortunately, ERH values calculated by Hypo71 (as the square root of the sum of the estimated latitude and longitude variances) indeed lack an inherent statistical interpretation (Boyd and Snoke 1984; Husen and Hardebeck 2010) and are generally smaller than the actual ERH.

ERH values reported by Mezcua and Martínez Solares (1983) are in the order of several kilometres to tens of kilometres and tend to decrease along time. In the early digital catalogue, the mean reported ERH is $\sim$ 7 km during 1983–1984, $\sim$ 4 km in 1985 and $\sim$ 3 km from January 1986 to October 1997. The marked reduction of ERH in the mid-1980s is explained by the deployment of the telemetred network and the increasing number of phases used for locating each event.

ERH values tend to be smaller onshore the Iberian Peninsula than elsewhere, evidencing that location uncertainty increased with the epicentral distance from the network (Fig. 5; for this kind of map see, e.g. Zaliapin and Ben-Zion 2015).

Since November 1997, epicentral location uncertainties calculated by Evloc are reported as error ellipses at 90 % confidence level in the full-format catalogue. In the absence of systematic location biases, the true epicentres would be expected to be inside such ellipses in 90 % of instances. Reported uncertainties reach the lowest values within the Iberian Peninsula and worsen rapidly offshore as the distance from the network increases (Fig. 6). Rueda Nuñez (2006, pp. 150–151), calculated theoretical values of the semi-axis of the error ellipse, in the Iberian region,
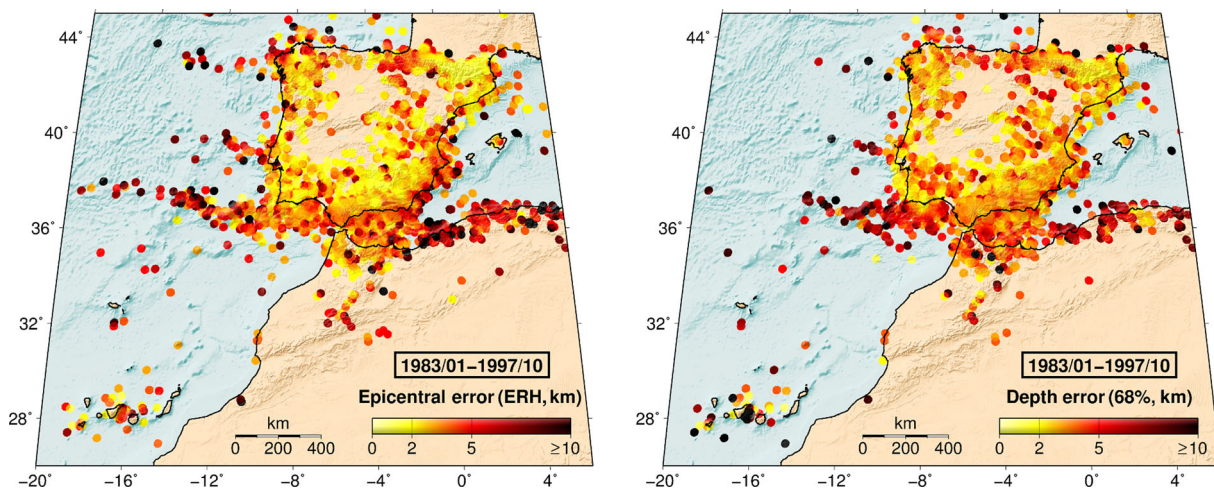
Fig. 5 Precision of hypocentral locations from January 1983 to October 1997. *Left:* Epicentral location errors (ERH values). *Right:* Hypocentral depth errors (68 % confidence ranges). Each location in the map shows the average value for the events with epicentres within a radius of 20 km

for $M = 3.0$, and considering the stations of the real-time IGN network then in operation. In general, those values and their spatial pattern are very similar to the results of Fig. 6. But in regions like the Pyrenees and Portugal, location uncertainties are typically lower than calculated by Rueda Núñez (2006) thanks to the data contributed to the catalogue by other networks (see also Souriau et al. 2014, for the Pyrenees).

In the Canary Islands, location uncertainties are generally higher than in the Iberian Peninsula. Azimuthal gaps are frequently large because the network geometry is constrained by the locations of the islands themselves. Moreover, noise level on the stations is relatively high (D'Alessandro et al. 2013), so the small earthquakes are typically detected by few of them. Further insight on location precision for specific
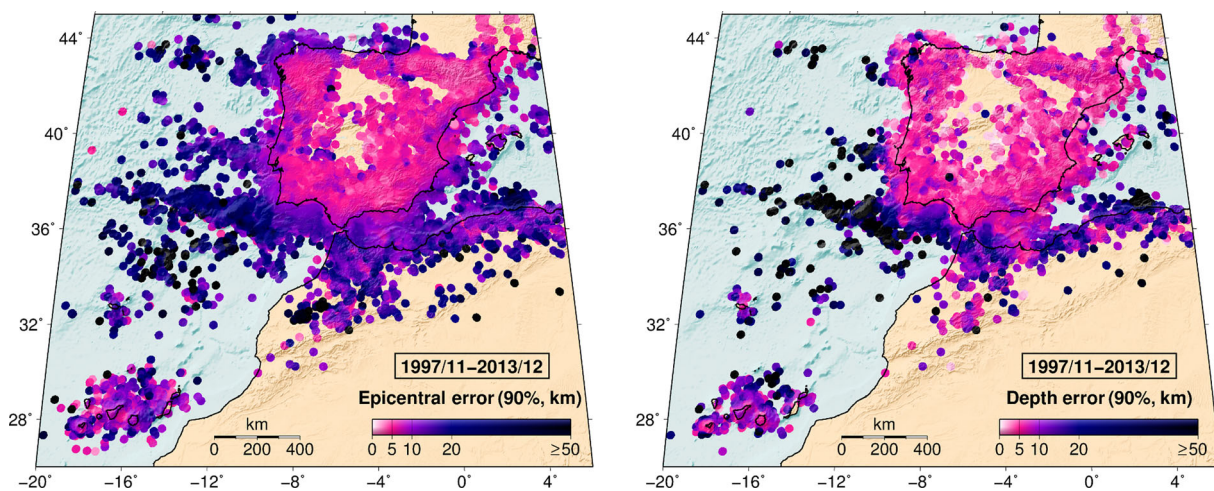

Fig. 6 Precision of hypocentral locations from November 1997 to December 2013. *Left:* Epicentral location errors (lengths of semi-major axes of the 90 % confidence ellipses). *Right:* Hypocentral depth errors (90 % confidence ranges). Spatial averages are calculated as in Fig. 5, but the errors were reported differently in the catalogue, hence the different colour scale used

earthquake series in the Canary Islands can be found in the relocation studies by Domínguez Cerdeña 2011, 2014).

3.3 Focal depth

Most of the seismicity in the catalogue is shallow (with focal depth $\leq$ 30 km for $\sim$ 93 % of events whenever calculated), but a fringe of intermediate-depth events (depth between 30 and 170 km) extends along the Iberian-African plate boundary (e.g. Buforn et al. 1997; Carreño 2003, Fig. 1). Also, since 1954, six deep earthquakes (depth > 600 km) have been recorded below the Granada region, in the South of the Iberian Peninsula (Frohlich 2006; Buforn et al. 2011; Bezada and Humphreys 2012; Mancilla et al. 2012, and references therein).

No focal depths are reported in the IGN catalogue for events whose epicentre is determined by macro-seismic means. Depth begins to be reported for a minority of earthquakes of the 1950s (Mezcua and Martínez Solares 1983). In the abridged catalogue, it is rounded off to the nearest kilometre, while in the full-format catalogue since November 1997, it is rounded off to the nearest tenth of kilometre. The evolution of reported depth versus time can be observed in Fig. 7.

For a large proportion of earthquakes (e.g. ~37 % since November 1997), the independent calculation of depth does not converge and fixed depth values are used (highlighted in Fig. 7), which restricts the location procedure to calculating the epicentral coordinates. Fixed depths, despite being the least constrained ones, have no reported uncertainty. Since November 1997, fixed depths are flagged as such in the full-format catalogue and omitted in the abridged version. Fixing depths has been proportionally more common in the earlier years (clearly until 1989 in the Iberian Region) and for small earthquakes (typically located with few stations) in more recent times. From 1983 until October 1997, the most usual value of fixed depths was 5 km, while since November 1997, it is 0 km, followed by 5 km and its multiples.

In the Iberian Peninsula, from January 1992 to October 1997, no depths $\gtrsim$ 70 km are reported, except for the 1993 deep earthquake (Fig. 7). Considering the depth distribution in the rest of the catalogue, from 1962 to 2013, this gap seems unlikely to be natural. Rather, it may be related to the location procedures used only during this period (Section 2.8). Depths $\gtrsim$
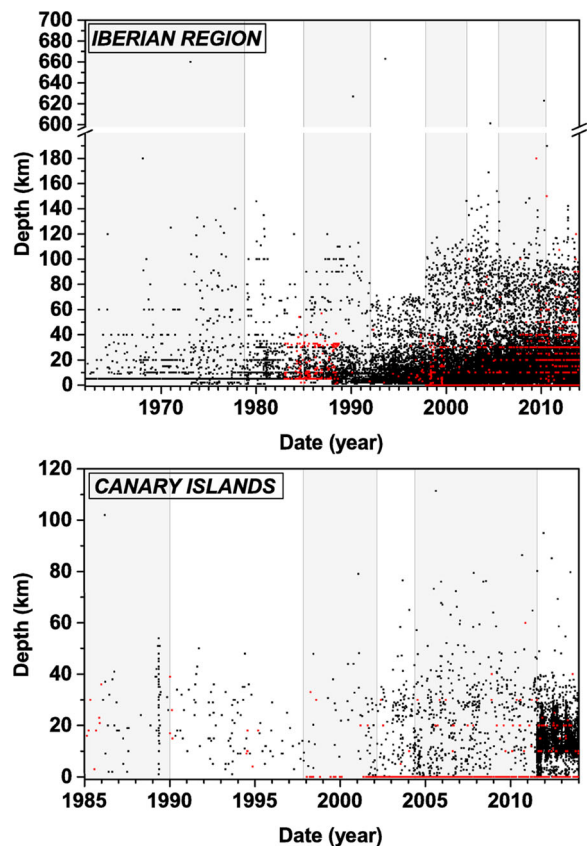

Fig. 7 Reported hypocentral depth versus time (*dots*). *Red dots* indicate the depths reported as fixed, that is, not calculated as independent parameters (the distinction is only available from 1983 onwards). *Vertical fringes* indicate the periods considered for completeness assessment. Geographic areas are those shown on maps of Figs. 12 and 14. In the Iberian Region, note the scale break between 200 and 600 km, where no value is reported in the catalogue

70 km were not reported again until November 1997 (Fig. 7), when improved automatic location routines became implemented.

Figure 5 shows the spatial distribution of reported hypocentral uncertainty from 1983 to October 1997. This uncertainty, calculated by Hypo71, can be interpreted as a 68 % confidence interval (Boyd and Snoke 1984; Husen and Hardebeck 2010). For this period, depth determinations tend to be better in the Iberian Peninsula than offshore and in distant areas, and are generally poor in the Canary Islands, such as for the earthquake series between Tenerife and Gran Canaria in 1989.

The geographic pattern of depth uncertainties is very clear since November 1997 (Fig. 6). These are

calculated with Evloc and reported as a 90 % confidence interval in the full-format catalogue. Onshore the Iberian Peninsula, and close to its coast, they are typically ∼ 5 km. Further away, they rise rapidly in proportion to the distance from the network. Beyond ∼ 150 km from the coast in the Atlantic (and offshore the Algerian coast), depths are mostly unconstrained (typical 90 % uncertainties are > 50 km). In the Canary Islands, reported depth uncertainties are heterogeneous, and usually larger than for the Iberian Peninsula. Uncertainties reported for the El Hierro earthquake series are typically low, thanks to the detailed monitoring (Section 2.13).

Focal depth is the most difficult spatial parameter to constrain (e.g. Vere-Jones 1992; Carreño et al. 2003; Husan and Hardebeck 2010), but in some regions the typical 90 % depth uncertainties seem lower than the epicentral ones (Fig. 6). The reason is that the highest depth uncertainties (those for fixed depth values) are not reported in the catalogue and cannot be considered in the corresponding maps (Figs. 5 and 6), so these have an optimistic bias.

4 Magnitude determination and precision

The magnitudes reported in the current version of the IGN catalogue have been calculated by using a variety of formulae, which are reviewed in this section, alongside the resulting uncertainties. These formulae have changed throughout time, and different ones were used in the original IGN bulletins before 1981 (López and Muñoz 2003).

Magnitude values are reported in the catalogue only for earthquakes with sufficiently reliable instrumental records. No magnitudes based on macroseismic information are provided, although they have been determined elsewhere for several historical or early instrumental earthquakes (e.g. Samardjieva et al. 1999; Martínez Solares and Mezcua 2002; Mezcua et al. 2004; Storchak et al. 2013). The first magnitude value (=6.4) is listed for the 26 June 1910 Masqueray (Algeria) earthquake. As the records improved during the twentieth century due to instrumental updates, magnitudes could be calculated and reported for a progressively larger proportion of earthquakes (Fig. 2), and all events occurred after 1989 have a magnitude assigned.

The reported magnitudes are, where possible, averages of the values obtained from a number of stations in a diversity of azimuths around the epicenter (Rueda 1995). Such averaging tries to counteract the variability of magnitudes calculated at different sites, which is due to the original radiation pattern, the attenuation and scattering along each particular ray path, and the diverse local site conditions which may cause local attenuation or amplification (e.g. Rueda 1995; Vila et al. 2005).

The full-format catalogue (Section 2.14) reports the standard error of the mean magnitude for each event. Note that when only one station is used this error cannot be calculated, but is reported as zero. From November 1997 onwards, when the magnitude was calculated from the phase picks of two or more stations, the mean standard error is ∼ 0.2 magnitude units. Magnitudes in the catalogue are rounded to one decimal place, which sets a precision limit of 0.1 units.

Different magnitude types can be reported for the same event, the preferred type being the only one reported in the short catalogue version (Section 2.14).

4.1 M_D, Iberian Region (1910–1961)

A duration magnitude (M_D) is reported for earthquakes in the Iberian Peninsula and surroundings, from 1910 to 1961 (before the installation of the first WWSSN station in 1962), taken from Mezcua and Martínez Solares (1983). It is based on the duration of the earthquake as recorded on at least one of three reference observatories (Toledo, Almería and Alicante), where the original mechanical seismographs operated for decades. A specific formula was used for each observatory (Mezcua and Martínez Solares 1983; Samardjieva et al. 1999):

$$M_D = 1.67 \log D + 0.001 \Delta - 0.2 \qquad \text{(Toledo),(1)}$$
$$M_D = 1.22 \log D + 0.001 \Delta + 1.20 \quad \text{(Almería), and(2)}$$
$$M_D = 1.44 \log D + 0.001 \Delta + 0.95 \quad \text{(Alicante),(3)}$$

where D is the duration of the earthquake in seconds and Δ the epicentral distance to the station in kilometres. The duration was measured from the arrival of the P wave until the moment at which the earthquake signal was indistinguishable from the background noise (Mezcua and Martínez Solares 1983). These formulae

were calibrated by regression to body-wave magnitude values (m_b) provided by the U.S. National Earthquake Information Service for a set of reference earthquakes. Mezcua and Martínez Solares (1983) state that the average standard error of these magnitude values is < 0.4.

4.2 M_D, Canary Islands (1964–1997)

In the Canary Islands, a duration magnitude was used until October 1997, using the formula (Rueda 1995):

$$M_D = 2 \log D + 0.0035 \Delta - 0.87. \qquad (4)$$

where D is the duration of the earthquake in seconds and Δ is the epicentral distance in km.

At the time of this writing, the magnitude type for these earthquakes in the catalogue is incorrectly labelled as if it were m_{bLg} (*sensu* Mezcua and Martínez Solares 1983, see below). No measurements of precision of magnitude values calculated with this scale are available.

4.3 m_{bLg} (1962–present)

Most magnitude values in the catalogue are provided in a m_{bLg} scale, a body wave magnitude estimated from the peak vertical motion of the *S*-wave, which at regional distances in continental crust typically occurs in the *Lg* phase (for the phase definition, see Storchak et al. 2003).

The *Lg* wave propagation may be blocked for several reasons, such as crustal scattering or a wave path through a thin, oceanic, crust (e.g. Chazalon et al. 1993; Calvert et al. 2000; McNamara and Walter 2001; Sens-Schönfelder et al. 2009; Noriega et al. 2015, and references therein). This may lead to m_{bLg} being underestimated with respect to M_w for offshore earthquakes (Cabañas et al. 2015). A clear example is the 26 May 1975 North Atlantic earthquake, with $M_w = 7.8$ (Storchak et al. 2013), but a much smaller m_{bLg}(IGN)= 6.7.

Two different scales of m_{bLg} have been used in the catalogue, for different periods, as described below.

m_{bLg} (1962–2002) In the printed IGN bulletins, this m_{bLg} was usually denoted simply as m_b. These formulae were used (Mezcua and Martínez Solares 1983; Rueda 1995):

$$m_{bLg} = \log\left(\frac{A}{T}\right) + 1.05 \log \Delta° + 3.90 \text{ for } \Delta° \leq 3°, \text{ and}$$
$$(5)$$

$$m_{bLg} = \log\left(\frac{A}{T}\right) + 1.66 \log \Delta° + 3.30 \text{ for } \Delta° > 3°,$$
$$(6)$$

where $\Delta°$ is the epicentral distance in geocentric degrees, and A and T are, respectively, the peak ground amplitude in microns, and the period of peak motion in seconds, of the *Lg* wave.

Mezcua and Martínez Solares (1983) calibrated Eq. 5 using the same reference earthquakes as for the M_D scale described before for the Iberian Region. Equation 6 is the formula adopted by the International Association for Seismology and the Physics of the Earth's Interior (Båth 1969, 1981), discussed by Nuttli (1973), Samardjieva et al. (1999), and references therein.

López and Muñoz (2003) pointed out that Eqs. 5 and 6 are not continuous to each other; there is a −0.34 unit fall at the epicentral distance of 3° (about 334 km), implying a relative underestimation of m_{bLg} for events occurred at larger distances from the station (Fig. 8).

Several regressions correlating this m_{bLg} with other magnitude scales were calculated by López Casado et al. (2000), Rueda and Mezcua (2002), Mouayn et al. (2004) and Cabañas et al. (2015).

From November 1997 to February 2002, the mean standard error reported for this magnitude scale is 0.1. Uncertainties for earlier events are not available; Cabañas et al. (2015) assigned by expert judgement values of 0.3 magnitude units before 1985 and 0.2 between 1985 and 2002.

m_{bLg} (2002–present) A new, improved m_{bLg} formula (López 2008) replaced the previous ones in 2 June 2003 for real-time magnitude determinations and was later applied retrospectively for all m_{bLg} calculations in the catalogue since 1 March 2002:

$$m_{bLg} = \log\left(\frac{A}{T}\right) + 1.17 \log R + 0.0012R + 0.67, \quad (7)$$
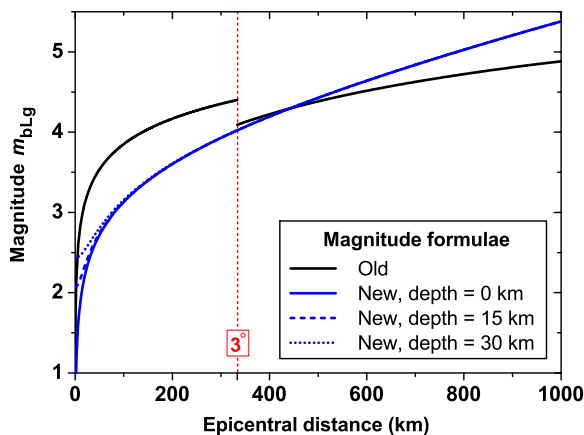
Fig. 8 Formulae used in the IGN catalogue to calculate the magnitude in m_{bLg} scale. The older ones (Eqs. 5 and 6, Mezcua and Martínez Solares 1983) had a break at an epicentral distance of 3° ($\simeq$ 334 km). The new one (Eq. 7, López 2008) is continuous and takes into account the hypocentral depth, though this effect is noticeable only for small epicentral distances. In the example shown, it is assumed that the peak ground amplitude (in microns) equals the corresponding wave period (in seconds). Other amplitude/period ratios would shift the curves vertically, but would maintain their relative differences

where A and T are the same as in Eqs. 5 and 6. R is the hypocentral distance in km:

$$R = \sqrt{\Delta^2 + h^2}, \tag{8}$$

where Δ is the epicentral distance and h the hypocentral depth, both in kilometres.

Equation 7 is substantially different from the older m_{bLg} formulae and implies a stretch of the magnitude range (Fig. 8). If an earthquake originates near most stations (at $\Delta < 3°$), its magnitude will tend to be lower than the one calculated by the old formulae. The opposite effect will result if the earthquake source is far from most stations (at $D \gtrsim 440$ km of epicentral distance).

Cabañas et al. (2015) calculated a regression between this m_{bLg} and M_w. The mean standard error reported for this magnitude scale in the catalogue is $\simeq 0.2$.

4.4 m_b, 1997–present

Since November 1997 in the Iberian region, and since November 2003 in the Canary Islands, for those earthquakes in which the Lg wave train is not apparent (in principle for those whose rays have oceanic paths $\geq 2°$, Carreño 1999), and for those with hypocentral

depth > 30 km (Cabañas et al. 2015), m_b, a body-wave magnitude calculated according to Veith and Clawson (1972) is used:

$$m_b = \log\left(\frac{A}{T}\right) + P(\Delta°, h) \tag{9}$$

where A is the maximum amplitude of a P type phase (Pn or P) in nm (Carreño 1999); T is the corresponding period in seconds and $P(\Delta°, h)$ is a correction factor (Veith and Clawson 1972) which depends on the epicentral distance $\Delta°$ in degrees and the hypocentral depth h in kilometres. This magnitude was calibrated for short-period vertical-component seismograms (Veith and Clawson 1972) although it is also being used with the seismograms from broadband stations (Martínez Solares et al. 2013). Cabañas et al. (2015) calculated a regression between this scale and M_w and noted that this m_b is systematically higher than M_w. Regressions to other regional magnitude scales were proposed by Mouayn (2007) and Peláez et al. (2012).

Between November 1997 and February 1998, m_b was used for few earthquakes only, while m_{bLg} was used for most. Almost all magnitudes during this period are labeled indistinctively as m_b, and the actual type of magnitude has to be deduced by checking, in the full-format catalogue, the type of phase used for magnitude determination. The mean standard error reported for m_b from March 1998 (when correct magnitude labelling starts) to December 2013 is $\simeq 0.2$.

Figure 9 shows the geographical distribution of epicenters from March 2002 to the end of 2013 where m_b is the preferred magnitude estimate. Indeed, most of them are located far from the Iberian Peninsula, Canary Islands or Balearic Islands (so the Lg waves had a relatively long path through thin crust before reaching the Spanish stations) and/or had deeper hypocenters (compare with the distribution of seismicity in Fig. 1).

4.5 M_w (2002–present)

For earthquakes with $m_{bLg} \gtrsim 3.5$ occurred since 2002, the moment magnitude, M_w (Hanks and Kanamori 1979), and moment tensor are calculated (Rueda and Mezcua 2005) with Dreger and Helmberger's method (1993) and reported in the abridged IGN catalogue (not in the full-format one). The detailed moment tensor results are reported in a separate catalogue online
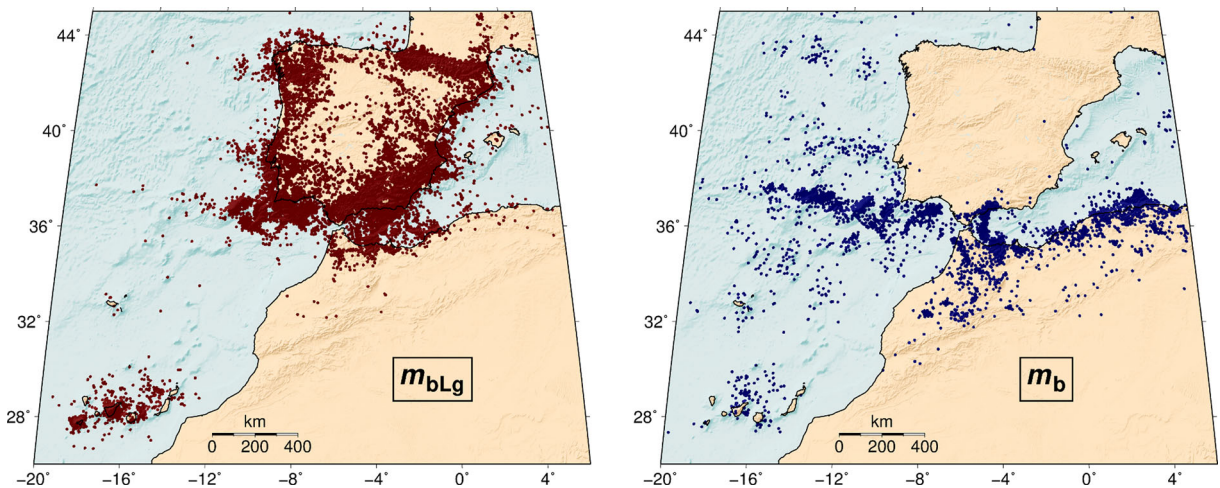
Fig. 9 Geographic distribution of epicentres from March 2002 to the end of 2013, separated by their preferred magnitude type (the one reported in the abridged catalogue online). *Left: m*bLg.

*Right: m*b. Only few earthquakes had M_w as the preferred magnitude during this period (not shown; see maps in Cabañas et al. 2015)

(IGN 2016a). The IGN catalogue also reports M_w for a few earlier earthquakes, taken from the literature (e.g. Battlló et al. 2008). Complementary M_w and moment tensor catalogs in the region are those of Stich et al. (2010), Martín et al. (2015) and references therein. The M_w values determined by IGN are usually similar to those by other authors, when available (e.g. Chevrot et al. 2011; Cabañas et al. 2015).

4.6 Evolution of magnitude values in the catalogue

The overall pattern of the magnitudes throughout time is shown in Fig. 10. A running median magnitude is calculated for each of the two regions analysed. For both, there is a decreasing overall trend, correlative with the general improvement of the network, which allowed detecting and recording smaller earthquakes.

In the Iberian region, at the beginning of November 1997, the median magnitude dropped by ∼ 0.5 units. This effect cannot be due to the introduction of m_b since initially almost all earthquakes still used m_{bLg}. Moreover, m_b are typically higher than m_{bLg} (see Cabañas et al. 2015), so the opposite effect in the median magnitude would be expected. This sudden decrease must be due to the increased reporting of smaller earthquakes thanks to the new automatic procedures for detection and location then implemented (Section 2.10), and the resulting increase in the number of phases used for location (Section 3.1). This

would also explain the slight increase in the rate of earthquakes detected since that date (Fig. 2).

In March 2002, the introduction of the new m_{bLg} formula caused two effects (see Gulia 2012, for similar issues in other catalogues). First, as expected (Section 4.3), it stretched the magnitude range reported. Second, it caused a drop in the median magnitude, because most earthquakes occurred close to the stations and were assigned lower magnitude values than with the old formula (Fig. 8). Both effects may have been intensified by the increasing ability of the broadband network to detect small earthquakes nearby and moderate earthquakes far away.

Brief, transient decreases of the running median are due to the recording of earthquakes with particularly low magnitudes close to seismic stations. For example, the swarms of low-magnitude earthquakes in Loja (1985) and Villanueva de Algaidas - Antequera (1989) took place in locations with relatively dense monitoring (Carreño et al. 1991a; Posadas et al. 1993), leading to a global decrease of the running median magnitude.

Conversely, distant sequences where most small earthquakes are undetected tend to cause sharp increases of this running median. The clearest examples are due to large earthquakes in northern Africa and their aftershock sequences, such as: 10 October 1980 El Asnam (now Chlef, Algeria), 21 May 2003 Zemmouri (Boumerdes, Algeria), 24 February 2004 Al Hoceima (Morocco), as well as abundant moderate
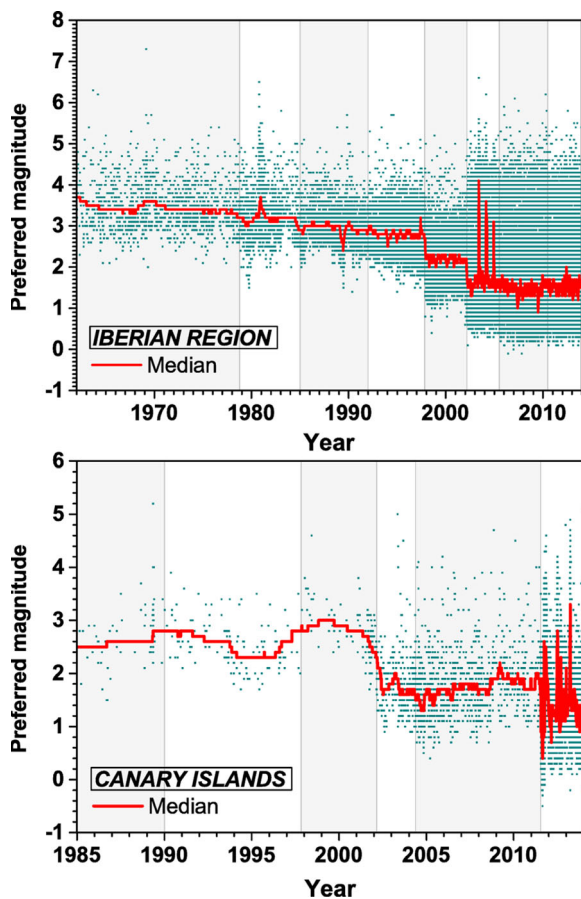
Fig. 10 Preferred earthquake magnitudes (i.e. those from the abridged catalogue version, Section 2.14) and their running median, for each region analysed (Figs. 12 and 14). In the Iberian region, the running value of the median magnitude is calculated with 200 earthquakes. In the Canary Islands, due to the scarcity of earthquakes before 2011, it is calculated using 50 earthquakes. *Vertical fringes* indicate the periods considered for completeness assessment

earthquakes south of Nador (Morocco) starting in late 2004.

In the Canary Islands, very few magnitude values are reported before 1985 (not shown in Fig. 10). In November 1997, there was an increase in the reported magnitude values, correlative to the replacement of the M_D scale by the old m_{bLg}. A clear decrease of about a magnitude unit in the early 2000s must be due to the deployment of the first broadband stations and the use of the new m_{bLg} scale since March 2002. From mid-2011 onwards, successive swarms at the island of El Hierro, monitored by a dense local network, yielded recordings of numerous small earthquakes and a complicated pattern of the running magnitude median.

5 Magnitude of completeness

The magnitude of completeness (M_c) is the lowest magnitude at which all earthquakes are detected and included in the catalogue (e.g. Rydelek and Sacks 1989; Wiemer and Wyss 2000; Woessner and Wiemer 2005; Mignan and Woessner 2012). An earthquake can be located if its signal is detected above the noise level at a minimum number of stations.

For a given network, a theoretical detection threshold (minimum magnitude which can be reliably detected) can be calculated and mapped for each location, considering the network geometry, the noise level at each station, the minimum number of stations required to detect and locate an earthquake, and the attenuation of signal amplitude with distance. For the Spanish National Seismic Network, Rueda and Mezcua (2006) provided a software to calculate such a threshold based on the detection of the Lg wave, and D'Alessandro et al. (2013) applied a more complex simulation-based method. But the IGN catalogue is not only compiled using the real-time backbone network (Figs. 4 and 14). Stations from other networks are also eventually considered for calculating final earthquake locations (Section 2.14). So theoretical detection thresholds are relevant to real-time network capabilities, but may be higher than the magnitude of completeness of the expanded and revised catalogue.

Here, M_c was calculated and mapped in successive periods using only the earthquake catalogue itself, as detailed below. The Iberian Region and the Canary Islands were analysed separately, considering the catalogue differences between them. The Online Resource 2 reports, for each location and period, the average M_c, its standard deviation δM_c and the resolution of the spatial sampling used.

5.1 Method used to calculate M_c

Seismicity commonly follows an exponential magnitude-frequency distribution (Ishimoto and Iida 1939; Gutenberg and Richter 1944):

$$\log_{10}[N(\geq m)] = a - bm, \quad \text{for } m \geq M_c. \quad (10)$$

where $N(\geq m)$ is the number of earthquakes with magnitude $\geq m$, and a and b are parameters. For $m < M_c$, $N(m)$ is lower than expected from the extrapolation of Eq. 10. This departure can be blamed

on catalogue incompleteness (e.g. Båth [1981]; Kwiatek et al. [2010]), since small-magnitude earthquakes are less likely to be detected (e.g. Schorlemmer and Woessner [2008]) and thus are preferentially missing. Several objective methods have been proposed to calculate the precise magnitude at which such a departure begins, albeit they do not always agree with each other (e.g. Mignan and Woessner [2012]; Michael [2014]; Roberts et al. [2015]).

Here, the Entire Magnitude Range method (EMR) was chosen, because of its proven reliability with small samples (as low as 60 earthquakes, Woessner and Wiemer [2005]). It is available in the free software ZMAP (Wiemer [2001]) and R (Mignan and Woessner [2012]). This method is computationally intensive and calculates M_c by fitting the entire range of the observed magnitude-frequency distribution (both the complete and the incomplete part). For $m < M_c$, a cumulative normal (Gaussian) distribution function is used, with mean μ and standard deviation σ. For $m \geq M_c$, Eq. [10] is fitted using a maximum-likelihood technique (Aki [1965]; Utsu [1965]), which is more robust than the least-squares method (Sandri and Marzocchi [2007]). The most likely value of M_c is provided by the best fitting model, which maximizes the log-likelihood function for the four parameters: μ, σ, a and b. The EMR method is somewhat conservative, as it may overestimate M_c in some cases (Mignan [2012]). For caution, I should note that for determining b reliably, a larger sample of earthquakes would be required (preferably at least 200 with $m \geq M_c$, Schorlemmer et al. [2005]; Roberts et al. [2015]).

To calculate M_c and its uncertainty in a robust way, bootstrap resampling (Efron [1979]) was used, following Woessner and Wiemer [2005]. Each sample of earthquakes was resampled with replacement 200 times, and M_c was calculated for each resulting bootstrap sample. This figure is high enough to obtain a stable average M_c and its standard deviation δM_c (Woessner and Wiemer [2005]), exemplified in Fig. 11. The presence of quarry blasts in the sample (Cattaneo et al. [2014]), changes in the b-value (e.g. Cesca et al. [2013]), or the mixture of magnitude scales may worsen the fit quality and increase δM_c.

5.2 Spatial sampling

The magnitude of completeness is spatially variable, mainly because it increases with the distance to
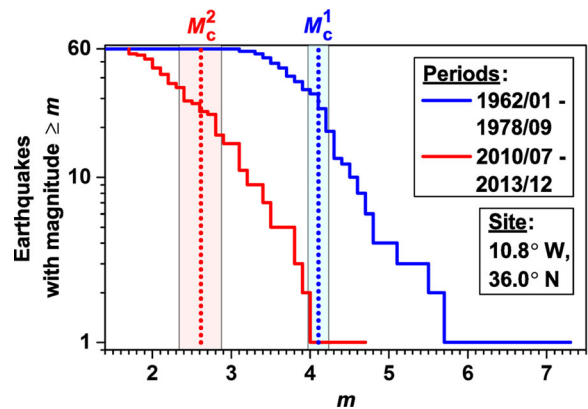

Fig. 11 Example of magnitude of completeness (M_c) and its standard deviation (δM_c) for a site in two different periods. This site is the closest node in the map to the largest earthquake of the catalogue in the instrumental era (28 February 1969, offshore Portugal, $m_{bLg} = 7.3$). *Solid lines* indicate the magnitude-frequency distributions of the closest 60 earthquakes to the node in the periods indicated. *Dotted lines* indicate the M_c calculated automatically with the EMR method (Woessner and Wiemer [2005]). *Colour bands* indicate the range of M_c plus/minus the δM_c calculated by bootstrap. The distribution is more gradually curved in the second period, leading to a larger δM_c. These values of M_c and δM_c are mapped at this node in the corresponding periods in Figs. [12] and [13] respectively

the network stations (e.g. Wiemer and Wyss [2000]; Schorlemmer and Woessner [2008]; Schorlemmer et al. [2010]). To account for this heterogeneity, here M_c was mapped locally, using a variable resolution, so that the resulting map is more detailed in the areas were more earthquakes were recorded.

A latitude-longitude grid was used, following Wyss et al. ([1999]) and e.g. Wiemer and Schorlemmer ([2007]) and Nanjo et al. ([2010]). The spacing between grid nodes was chosen as 0.1° both in latitude and longitude, on the order of the epicentral location uncertainties (Section [3.2]). For each node, M_c and δM_c were calculated using its closest earthquakes, at least 60. Distances were measured along the great-circles between the nodes and the epicentres, using a spherical model for the Earth, with radius 6371.007 km, the sphere of equal area of the most frequently used Earth reference ellipsoids (Moritz [2000]; NIMA [2000]). Initially, a search radius of 5 km around each node was considered (so that the search area is similar in size to the latitude-longitude cells of the grid). If there were < 60 epicentres within this radius, it was increased until it included the 60 closest earthquakes, but up to a maximum of 100 km. This limit attempts to avoid

mixing earthquakes from regions too distant to each other, with different M_c (e.g. Nanjo et al. 2010) and to minimize the artifact of calculating it in areas devoid of earthquakes.

In the resulting map, the blank regions have too few earthquakes recorded per unit area to calculate a meaningful M_c (< 60 within 100 km from a node). Compared with the other regions, they have either an intrinsically lower seismicity rate, or a higher M_c, or both. For some regions, M_c could be calculated in periods with high seismicity rate (for example, with aftershock sequences) but not in others. It might be possible to extrapolate M_c to these blank areas using different procedures, which consider how it increases with distance from the stations (Schorlemmer and Woessner 2008; Mignan 2012). To properly use such methods, it would be necessary to know (or to deduce, e.g. Gentili et al. 2011) when each station was in operation and contributing data to the catalogue. In the IGN catalogue, this would be possible for the stations of the backbone network, but becomes exceedingly complicated for the additional stations from other institutions.

Since depths are often poorly determined, or not determined independently at all (Section 3.3), I chose not to set a fixed maximum depth threshold. Only the five earthquakes with depth > 600 km (Section 3.3 and Fig. 7) were excluded from the analysis. This is a conservative approach: deep earthquakes are less likely to be detected than shallow ones, so the M_c calculated from a sample with mixed depths will be higher than if only the shallow earthquakes were considered. In most areas, the catalogue is dominated by shallow seismicity anyway (Fig. 1 and Section 3.3), so except for specific locations discussed later, depth is probably a minor factor compared to the epicentral distance from the stations.

5.3 Choice of temporal periods and magnitude scales

To account for temporal heterogeneities in M_c, the catalogue was divided into periods. Ideally, these should be long enough to include many earthquakes, for calculating M_c in as many locations as possible, and reducing the extent of blank areas. But they should be short enough to ensure that M_c was stable, with a relatively stable network (e.g. Hutton et al. 2010) and without changes in magnitude reporting (e.g. Tormann et al. 2010). Using too long periods with unstable

completeness would yield underestimated M_c values, because the departure from Eq. 10 is controlled by the statistics of the most complete parts of the catalogue (e.g. Michael 2014).

Periods were separated by milestones in the development of the backbone network, improvements in the earthquake detection routines and changes of the magnitude formulae used. The evolution of other networks which contributed to the catalogue (either temporary ones or from other institutions) had to be disregarded to avoid exceeding complexity.

The preferred magnitude listed by IGN for each earthquake in the abridged catalogue was used. M_c at each node depends on the magnitude scale(s) used locally (e.g. Fig. 9). In the full-format catalogue, only one magnitude type is typically reported, so separating earthquakes by magnitude type would indeed create subsets less complete than the original catalogue. Thus, it is not statistically meaningful (although it would be more physically meaningful) to calculate M_c separately for each magnitude type. Reliable magnitude conversion formulae for this catalogue (Cabañas et al. 2015, and references therein) are not available for $M \lesssim 3$, while it was expected that $M_c < 3$ in most of the region, so I did not attempt to convert magnitudes to a common scale.

5.4 M_c in the Iberian Peninsula and surroundings

According to Mezcua et al. (2011) and Martínez Solares et al. (2013), the catalogue may be complete in the Iberian Peninsula for $M \gtrsim 5$ since the early nineteenth century, and for $M \gtrsim 4$ since the mid-twentieth century, being less complete offshore, in northern Africa, and in earlier times. These assessments estimated the missing magnitudes from macroseismic intensity and assumed that, for a given magnitude threshold, the catalogue is complete from the moment at which the earthquake rate from that threshold upwards becomes stationary (following Stepp 1972).

The analysis made here covers the years 1962 onwards, for which the catalogue reports magnitude systematically for most events. The increasing slope of the cumulative number of earthquakes (Fig. 2) and the overall decrease of the median magnitude (Fig. 10) already evidence that M_c in the catalogue has been reduced throughout the decades. Figure 4 shows maps with the backbone stations in each period, while M_c and δM_c are mapped in Figs. 12 and 13, respectively.
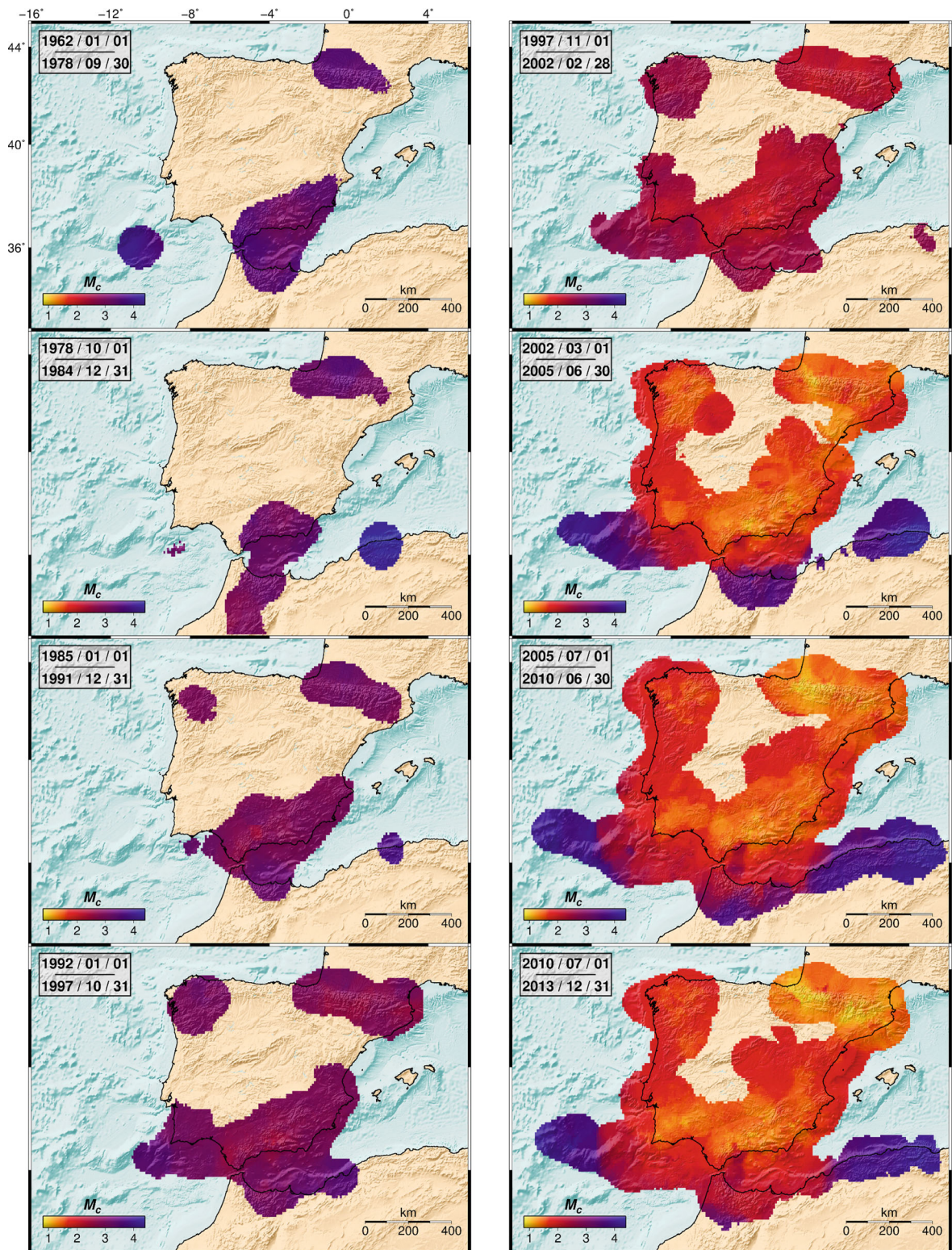
Fig. 12 Evolution of the magnitude of completeness (M_c) of the catalogue in the Iberian Peninsula and surroundings, in cylindrical equal-area projection, for the periods indicated. The data are provided in the Online Resource 2
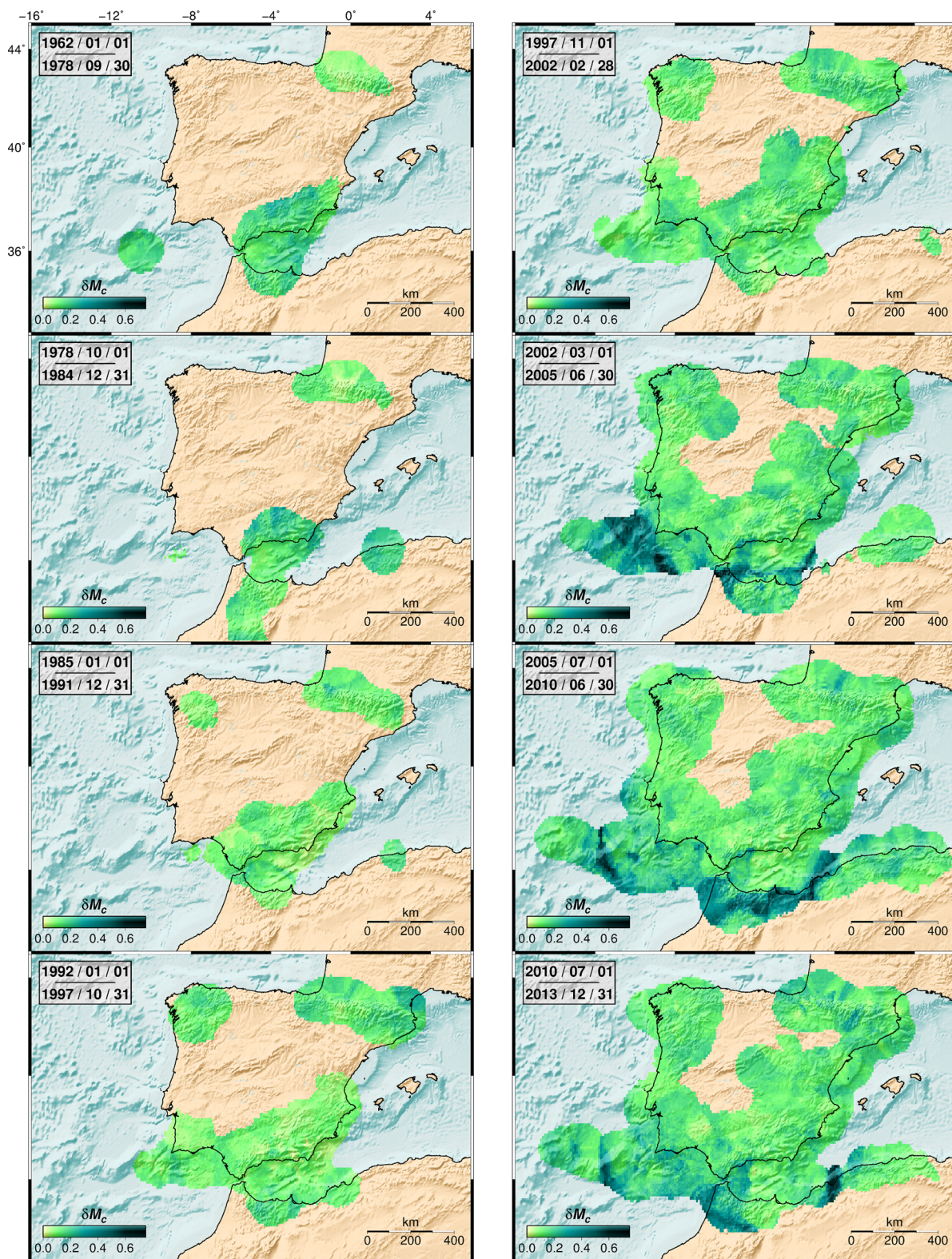
Fig. 13 Standard deviation δM_c of the magnitude of completeness mapped in Fig. 12. The data are provided in the Online Resource 2

During the first four periods considered (January 1962 to October 1997), a single m_{bLg} scale was used; relatively few earthquakes were recorded (Fig. 2) so M_c can be reliably determined only in the most seismically active areas.

The first period analysed is chosen to include from January 1962 (for which the m_{bLg} scale started to be used, Mezcua and Martínez Solares 1983) to September 1978, and during this time, only a few IGN observatories operated, including the WWSSN stations of Toledo and Málaga (these from late April 1962 onwards, ISC 2016a). M_c was 3.0–3.7 in the Alborán Sea (the westernmost corner of the Mediterranean) and its surrounding mountain ranges (Betics to the north, Rif to the south), while it was 3.2–3.5 in the Pyrenees. In the Atlantic Ocean, the location of the largest earthquake in the instrumental era, occurred in 1969, has the highest M_c determined in this period, $\simeq 4.1$ (see also Fig. 11).

During the initial deployment of the short-period, telemetred, Spanish National Seismic Network (October 1978 to December 1984) M_c improved slightly, but was still > 3 in the Iberian Peninsula. In NW Algeria, the catalogue is dominated by the 1980 El Asnam (now called Chlef) earthquake and its aftershock sequence, which were recorded with $M_c \simeq 4.5$.

During the first years of the new network (January 1985 to December 1991), and with an increasing number of stations, M_c decreased to < 3 in all areas where calculable in the Iberian Peninsula and immediate surroundings, reaching down to 2.4–2.6 at and around the location of the 1985 Loja swarm in the Betics, which was monitored by IGN with temporary stations (Carreño et al. 1991a). This swarm and others during this period caused a decrease of the median magnitude in the catalogue (Fig. 10 and Section 4.6). In the periphery of the network, such as on the northern side of the Pyrenees and in the Rif, M_c was still 3.0–3.3. Meanwhile, M_c dropped to ~ 3.7 at the same spot in NW Algeria mentioned in the previous period.

The catalogue is complete in the most seismic areas of the Peninsula down to $M_c \simeq 3$ since 1992. At that time, the first automatic location procedure was fully in operation (which also corresponds to a different pattern in depth reporting, Fig. 7 and Section 3.3), and since late 1992, the Sonseca array started providing data to the catalogue. Between January 1992 and October 1997, the best monitored areas continued to be in the SE of the peninsula, M_c reaching 2.3 locally, while M_c increased according to distance from the network, reaching 3.5 offshore to the SW of the peninsula, and in sites of northern Africa.

A major improvement of the catalogue completeness is observed from November 1997, when the new automatic location procedures were implemented. This was also evidenced by a sudden drop in the median magnitude (Fig. 10 and Section 4.6). Anywhere in the peninsula (where measurable) $M_c \leq 2.8$, and reached down to 1.7 precisely at the site with the densest monitoring, in the Granada region (Betics). Even the values calculated offshore and in northern Africa were $\lesssim 2.8$, which is surprisingly low. This may be attributed to the underestimation of m_{bLg} for distant offshore earthquakes (Section 4.3); m_b had started to come into use, but during this period only for $< 1\%$ of earthquakes, so with very slight influence on M_c.

The most dramatic drop in M_c took place since March 2002, which also corresponds to a drop in median magnitude (Fig. 10 and Section 4.6) and to the most remarkable increase in the apparent frequency of earthquakes with $M \leq 3$ (Fig. 2). This must be due both to the deployment of the new broadband network and to the use of the new, improved m_{bLg} formula, which provides lower magnitude values for earthquakes at epicentral distances $\lesssim 440$ km from the station (Sections 4.3 and 4.6). Between March 2002 and June 2005, $M_c \lesssim 2.0$ over the whole Iberian Peninsula, and typically $\lesssim 1.5$ in the most densely monitored areas, a pattern which continues along the broadband era. Despite the network improvement, M_c rose with respect to the previous period in locations far offshore and in regions in northern Africa, which is explained by the systematic use of m_b for distant earthquakes, that tends to provide higher magnitudes (this also occurs with the new m_{bLg} scale compared with the older one at distances $\gtrsim 440$ km).

Between July 2005 and June 2010, the broadband network continued to grow. Completeness improved noticeably in offshore areas. The greatest drop of M_c, down to $\simeq 1.0$ in the western Pyrenees, was due to the deployment of the dense network around the Itoiz and Yesa reservoirs (Section 2.12). Regions exist however, where stations were closed down (Fig. 4) and M_c worsened nearby, especially in Galicia (NW Iberian Peninsula) and other areas in the interior of the Peninsula.

During the last period analysed (July 2010 to December 2013), the completeness was similar to the previous one, although the progressive closing of almost all remaining short-period stations of the backbone network explain local deteriorations of completeness (such as around 3° W, 39° N).

The uncertainty of the results, δM_c (Fig. 13), is remarkably low (typically ≤ 0.2, i.e. in the order of the magnitude uncertainties themselves, Section 4). But a few exceptions during the broadband era require additional explanation. Offshore and in Northern Africa, a sharp transition from $M_c \simeq 2.5$ to $\gtrsim 3.5$ is measured, associated to the highest δM_c values (≥ 0.4). This must be due to the use of different magnitude scales (Fig. 9 and Section 4), with m_b values for the more distant earthquakes being systematically higher than the m_{bLg} values of similar, closer earthquakes (because of overestimation of m_b, Cabañas et al. 2015). So in the spatial fringes where the mixture of magnitudes takes place, the measured M_c changes abruptly, the theoretical fit to the magnitude-frequency distribution is poorer and with higher δM_c. In the Alborán Sea, a N-S area has higher M_c than the surroundings, and with relatively high $\delta M_c \sim 0.3$. Relatively abundant intermediate-depth earthquakes (plus shallow ones) take place here (Buforn et al. 1997). So, consequently, a local mixture of M_c ensues: the deeper earthquakes are being less completely recorded (and measured in m_b scale, both factors raising the overall M_c), while the shallower ones are more completely recorded (and in m_{bLg} scale). In other offshore areas, in the Atlantic, intermediate-depth earthquakes also take place, and a similar situation probably occurs, though less spatially localized.

In Peninsular Spain, within each period, M_c generally correlates with the distance to the stations shown in Fig. 4, and largely agrees very well with the theoretical detection thresholds of the Spanish National Seismic Network for specific dates. Maps of these thresholds, elaborated by IGN personnel and apparently based on the method implemented by Rueda and Mezcua (2006), are available for the network configuration ca. 1990 (Fig. 16 of Mezcua 1995), 1993 (Fig. 17 of Mezcua 1995), 2002 (Fig. 3 of Carreño et al. 2003) and 2010 (Rueda 2010, which does not include the dense network in the Aragón Valley). The most recent theoretical analysis of the detection threshold was made by D'Alessandro et al. (2013), assuming that all the stations listed in their

Table 1 were functioning simultaneously (Antonino D'Alessandro, pers. comm., 2013). That list, however, includes all stations ever operating in the backbone network, mixing stations that were opened up to mid-2010 with those already permanently closed. This prevents a meaningful comparison with such a detection threshold in most of the region. For the dense IGN network around the Itoiz and Yesa reservoirs, for which indeed the stations were simultaneously operating by mid-2010, the detection threshold (local magnitude $M_L \sim 1.0$) calculated by D'Alessandro et al. (2013) is like the M_c calculated there during the last two periods.

During the broadband era, M_c is lower than the expected detection thresholds (from Carreño et al. 2003; Rueda 2010) in the eastern Pyrenees (most notably since 2010), southern Portugal, several locations in Andalusia (southern Spain) and in NW Africa (with notable progressive improvements since 2005). These are areas where the catalogue truly benefits from the data from additional stations of other institutions within Spain and neighbouring countries, whose networks were also improving at the time. Conversely, M_c is higher than expected in the areas where m_b was predominantly used, because such theoretical detection thresholds were based on m_{bLg}.

5.5 M_c in the Canary Islands

In the Canary Islands, the catalogue seems quite incomplete before the ninetieth century (e.g. Vinciguerra and Day 2013) and even until the mid-1980s (only 67 earthquakes are listed from 1962 to 1984). An overview of the historical earthquakes was given by González de Vallejo et al. (2006). The Canary catalogue until 1980 is taken from Mezcua and Martínez Solares (1983), who warned that it is probably not valid for statistical analyses, since it relies on diverse partial sources, and they had to complement the instrumental observations during 1960–1980 with the bulletin of the International Seismological Centre. Given those limitations, I have chosen to calculate M_c only from 1985 onwards.

For each period considered for completeness analysis, the stations of the Spanish National Seismic Network, M_c and δM_c are mapped in Fig. 14. Several of the milestones used for separating periods are different than for the Iberian Region, given that the Canary subnetwork had a separate temporal evolution

Fig. 14 Evolution of the network and catalogue completeness in the Canary Islands. *Left:* Permanent IGN stations contributing to the catalogue, during the periods indicated. *Center:* Magnitude of completeness (M_c). *Right:* Uncertainty of the magnitude of completeness (δM_c). The colour scales are identical to those in Figs. 12 and 13, and the data are provided in the Online Resources 1 and 2
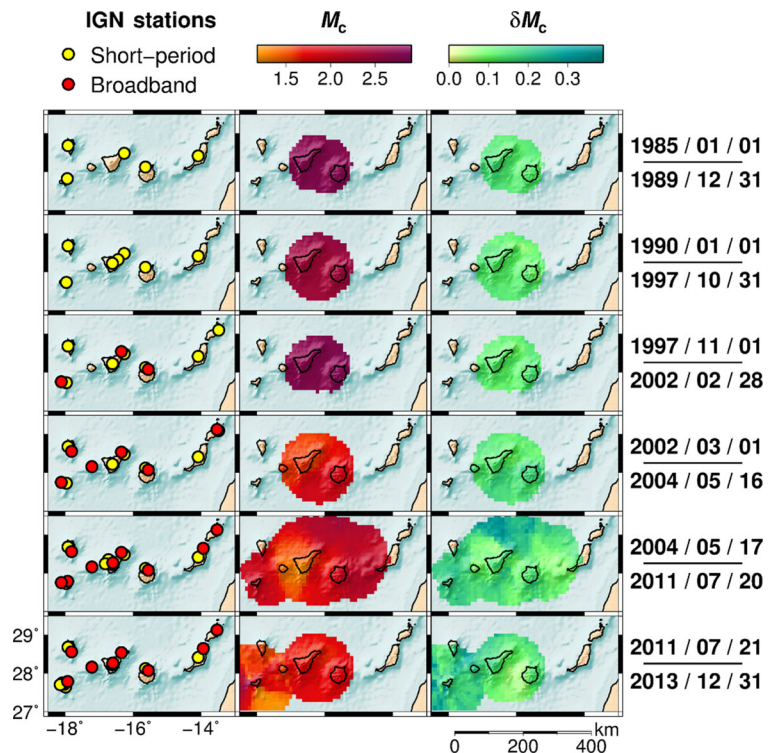
and that (as it comprises few stations) M_c may be notably influenced by each station opening or closing. Before the seismic swarms below El Hierro island, most of the seismicity had taken place near the center of the archipelago, especially between the two largest islands, Tenerife and Gran Canaria. Until May 2004, M_c can be calculated with sufficient spatial detail only in this central area, while later on there are sufficient earthquakes for measuring it over a wider region.

During the early years of the short-period telemetred network (1985 to 1989), M_c (in M_D scale, Section 4.2) was 2.7–2.8. The new stations opened in Tenerife in 1990 (Section 2.7) lowered M_c there to 2.4–2.6 from January 1990 until October 1997. From November 1997 until February 2002, the median magnitude rose (Fig. 10) and M_c also rose to 2.7–2.9, despite the new automatic location procedures. This worsening is partially due to the change in magnitude scale (to the older m_{bLg}), and probably also due to the closing of one of the three short-period stations in Tenerife in January 1997. Data from the first broadband stations during April 2001 to February 2002 reduced the median magnitude (Fig. 10) and probably reduced M_c, but this could not be measured as too few events were recorded during this brief period.

As in the Iberian region, M_c has been greatly reduced during the broadband era. The introduction of the new m_{bLg} scale in March 2002 (Section 4.6) and the deployment of the initial broadband network reduced M_c down to 1.5–2.0 until mid-May 2004. The new stations deployed since this date in Tenerife (Section 2.13) further lowered M_c to ~ 1.3 just below this island, while it rose outwards from there up to 2.4 at the farthest locations from the network.

In the last period considered, the catalogue is dominated by the seismicity in El Hierro, thanks partly to the dense seismic network there deployed since 21 July 2011 (Section 2.13). M_c below and around El Hierro is spatially heterogenous, with the lowest values (~ 1.2) to the south of the island, probably because that was the location of the shallowest hypocentres, close to the submarine eruption site (e.g. Domínguez Cerdeña et al. 2014). The apparent extension of these low M_c up to 100 km offshore SE of El Hierro, where actually no earthquakes were recorded, is an artifact of the spatial windowing procedure. West of El Hierro, where several swarms of more distant, deeper earthquakes took place after the eruption, is where the highest values (up to 2.9) are measured. During the swarms preceding the

eruption, the earthquake foci migrated significantly with respect to the network, and new stations were opened (Domínguez Cerdeña et al. 2014). These factors contribute to explain the temporal changes of M_c observed by Ibáñez et al. (2012) and Telesca et al. (2016). During the eruption, reported magnitudes were typically higher than before (e.g. Ibáñez et al. 2012, their Fig. 3B). This may be, at least partially, a consequence of the volcanic tremor of variable amplitude which accompanied the eruption and which hampered the detection of the smallest earthquakes. All the mentioned factors bring about a sense of the complexity of determining a meaningful M_c in the El Hierro earthquake series (see also Roberts et al. 2015). Meanwhile, two of the Tenerife stations were no longer in operation in this last period, what explains the increase of M_c there up to 1.6–1.8.

6 Daily and weekly variations

The seismic noise produced by human activities (vehicle traffic, machinery from industries, etc.) typically has daily and weekly cycles. It is higher during daytime than nighttime, and also higher on weekdays than at weekends (e.g. Bonnefoy-Claudet et al. 2006; Díaz et al. 2010; Custódio et al. 2014). Even a relative decrease of seismic noise is sometimes observed during lunch breaks (e.g. Bonnefoy-Claudet et al. 2006; Díaz et al. 2010). As a result, since the ability to detect and locate earthquakes decreases with noise amplitude, commonly more earthquakes are recorded in the catalogues during nighttime (e.g. Rydelek and Sacks 1989; Iwata 2013), lunch breaks (e.g. Custódio et al. 2015) and weekends (Zotov 2007; Atef et al. 2009).

Daily variations, with fewer detected events during the daytime hours attributable to higher artificial noise, are apparent in the catalogue (Fig. 15). This effect had already been reported by Carniel et al. (2008), Del Pin et al. (2008) and Domínguez Cerdeña et al. (2011) in the Canary Islands and by Custódio et al. (2015) in the Portuguese catalogue. The daily variation is less apparent during the period with volcano-tectonic episodes in El Hierro (not plotted in Fig. 15), indicating that recorded earthquake frequencies may then have been mostly dominated by natural, temporal variations of the seismicity rate.
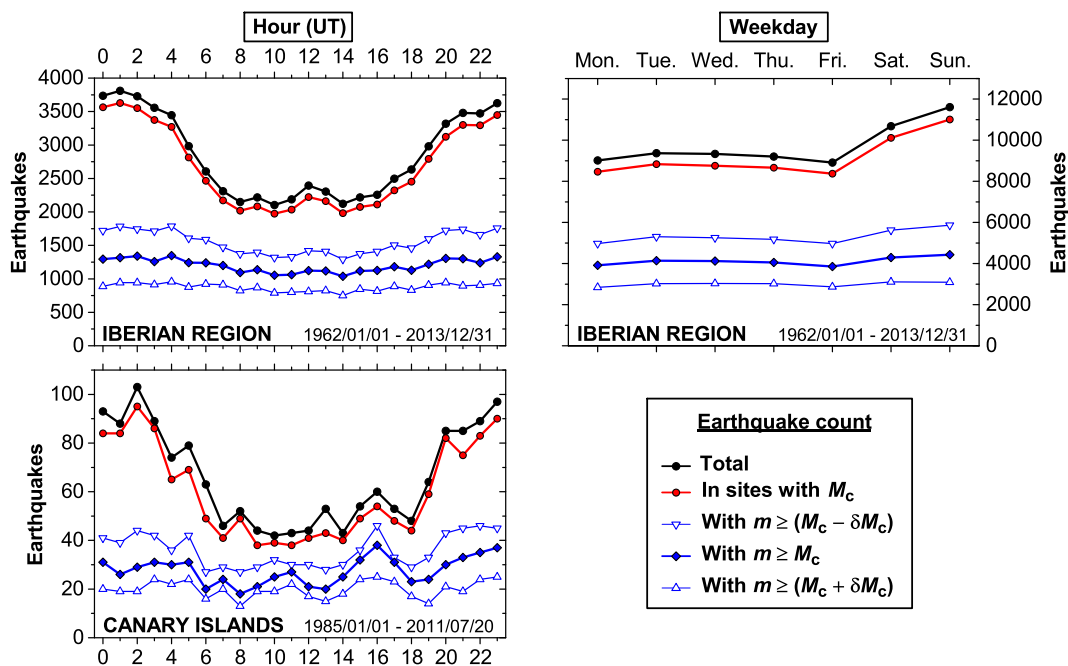

Fig. 15 Hourly and weekday earthquake frequencies in the Iberian region and Canary Islands (areas of Figs. 12 and 14) for the periods indicated. The magnitude of completeness M_c and its uncertainty δM_c are those at the specific time and location of each earthquake. Solar noon is around 12 h Universal Time (UT) in the Iberian Peninsula and 11 h UT in the Canary Islands

A slightly higher frequency of earthquakes is recorded around noon in the Iberian region. This could be attributed either to the effect of catalogue contamination by blasts detonated precisely during the lunch break (Section 7, see also Gulia, 2012) and/or to a lower M_c thanks to the lower artificial noise at lunchtime, as proposed for the Portuguese catalogue (Custódio et al. 2015).

A weekend effect is clearly observed in the Iberian region, with significantly more earthquakes being recorded on Saturdays and especially on Sundays (Fig. 15). In the Canary Islands, it is not observed (not plotted in Fig. 15 for simplicity), which might mean that artificial noise has a similar amplitude throughout the whole week.

Such cyclic effects should be smoothed out if only the complete part of the catalogue is considered, above a completeness threshold (e.g. Rydelek and Sacks 1989). To test this (and thus indirectly the reliability of the completeness analysis), I considered for each earthquake the local M_c and δM_c at the particular latitude-longitude cell and specific period at which the earthquake occurred (Fig. 15). Most earthquakes in the instrumental era took place in sites where completeness had been determined. If only earthquakes with $M \geq M_c - \delta M_c$ are considered (i.e. a low, optimistic, threshold), the daily and weekly variations are greatly reduced, but do not disappear completely, so the catalogue is not complete for that threshold. For $M \geq M_c$, these variations seem to vanish completely, and the remaining variability in earthquake frequency is probably real. The pattern is very similar if a higher, more conservative completeness threshold, $M \geq M_c + \delta M_c$, is used. These results support the completeness analysis, evidencing that the calculated M_c is the minimum threshold of completeness of the catalogue, and that its uncertainty, δM_c, is partially due to the daily and weekly variations in the noise level.

7 Catalogue contamination by blasts

Earthquake catalogues are often contaminated by artificial events, most frequently quarry or mine blasts (e.g. Wiemer and Baer 2000; Gulia 2010; Gulia et al. 2012; Cattaneo et al. 2014). Blasts misclassified as natural earthquakes alter the statistics made with the catalogue and may artificially rise the seismicity rate and the calculated seismic hazard. They are especially difficult to identify when they take place in seismically active regions.

The online IGN catalogue aims to only include natural earthquakes and to exclude artificial seismicity, a challenging task since the Iberian Peninsula hosts extensive mining activities. In the printed bulletins up to 1986, earthquakes identified as artificial explosions were still listed and specifically labelled. Artificial events are typically of low magnitude, so they started to become more frequently recorded since the 1980s. The reduction of M_c since the deployment of the broadband network in the 2000s (Section 5) enabled recording tens of thousands of blasts in the Iberian Peninsula, outnumbering by far the actual earthquakes (Rueda Núñez 2006; García Vargas et al. 2016). Routine screening relies on analyst judgment, based on waveform analysis and on the time of occurrence, being blasts expected preferentially during daylight hours (García Vargas et al. 2016).

Despite such efforts, artificial events occasionally pass this screening and are incorporated in the catalogue as if they were natural seismicity (García Vargas et al. 2016). For example, thanks to the use of a dense local network, Torcal et al. (2005) identified several explosions or quarry blasts which had been considered natural microearthquakes in the IGN catalogue. In a more generic analysis, Gulia (2010) identified sites with suspect contamination of quarry blasts in this and other European earthquake catalogues. Her analysis is based on the ratio of daylight to nighttime events, which takes into account that blasts at quarries or construction sites typically occur during daytime (e.g. Benson et al. 1992; Wiemer and Baer 2000; Gulia et al. 2012; Panzera et al. 2016), while natural earthquakes are typically more abundantly recorded in the catalogues during nighttime, because of the lower artificial noise (Rydelek and Sacks 1989, and Section 6).

An illustrative example of blast contamination highlighted by a high daytime to nighttime ratio is the Trimouns talc quarry (de Parseval et al. 2004), the largest open-pit talc mine in the world. It is located near Luzenac, in the French Pyrenees, where natural earthquakes also take place (42.805° N, 1.804° E, Fig. 16). Mining is carried out there from May to November, and blasting is performed at a very narrow time interval within the evening breaks, shortly before 16 h UT, that is 18 h summer official time (Julien Conté, former Trimouns mining project manager, pers.
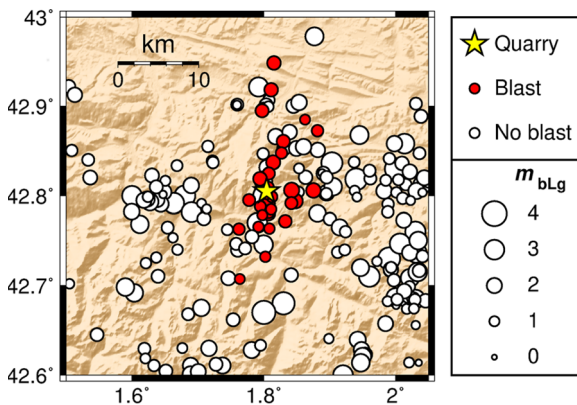
Fig. 16 Example of catalogue contamination by quarry blasts. *Star* indicates the location of the Trimouns talc quarry in the French Pyrenees. *Circles* indicate earthquakes recorded until December 2013, with size proportional to magnitude (m_{bLg} scale). *Red circles* indicate highly likely blasts, that is, recorded at the typical daily blasting schedule at this quarry (a narrow range of just 7 min, 15:50-15:56 UT) during different months and years. *White circles* indicate earthquakes recorded at other times, which are most likely natural seismicity. Digital elevation model from Farr et al. (2007)

comm., 2015; Godey et al. 2013). At this location, the IGN catalogue includes tens of highly likely quarry blasts, recorded in different years since 2004 with origin time between 15:50-15:56 UT, and $m_{bLg} \leq 2.0$ (Fig. 16).

The catalogue, however, offers examples of blast contamination with precisely the opposite pattern: a particularly high frequency of nighttime blasts.
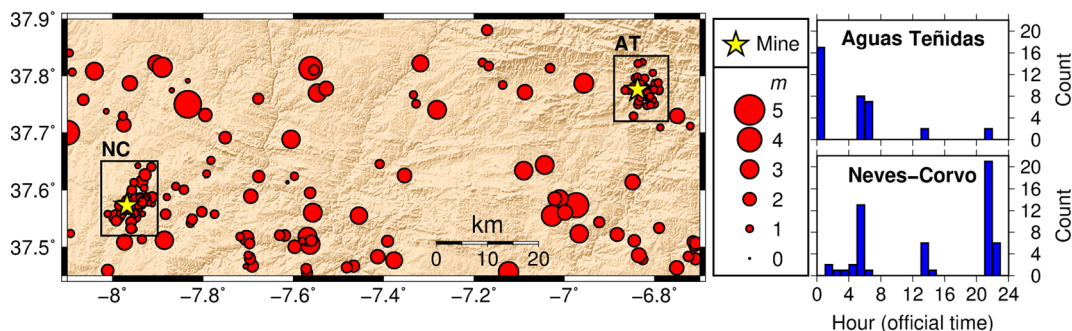
Figure 17 shows the seismicity in part of the Iberian Pyrite Belt, a geologic region rich in massive sulphide deposits (Leistel et al. 1998; Rosa et al. 2010), which is also seismically active. Two tight clusters of small-magnitude earthquakes ($m_{bLg} \leq 2.3$, and ~ 1 in most cases) pinpoint the Portuguese mine of Neves-Corvo and the Spanish mine of Aguas Teñidas, where sulphide ores (mostly of copper and zinc) are extracted after large-scale underground blasting (Chadwick 2007; García Maneiro et al. 2012). Neves-Corvo (currently the largest copper and zinc mine in the European Union) started operating in 1988, but seismicity is recorded in the catalogue only since 1999 (perhaps because this is about the time when the magnitude of completeness began to be low enough to record these small events, Fig. 12). At Aguas Teñidas, recorded seismicity began in 2009, right when commercial extraction started. Other earthquakes in the area may be tectonic, which underlines the need of distinguishing blasting from actual seismicity. In both mines, most recorded events occur in agreement with blasting schedules (Fig. 17). For the sake of safety, underground blasts are performed when workers are out of the mine (during meal breaks or shift changes). So they typically occur every 8 h (at early morning, lunch time and dinner time), and also around official midnight in Aguas Teñidas (Sheila Maqueda –former drill and blast engineer at this mine–, pers. comm. 2014). Finally, these mines are exploited (and earthquakes have also been recorded at them) all days of the week. These observations cast doubts on the

Fig. 17 Examples of catalogue contamination by underground mine blasts. *Stars* indicate the location of the mines of Aguas Teñidas (*AT*) and Neves-Corvo (*NC*), in SW Iberian Peninsula. *Circles* indicate earthquakes, with circle diameter proportional to magnitude ($m_D = 4.5$ for the largest event, and m_{bLg} scale for all the others). *Histograms* indicate hourly frequencies of the

earthquakes within the polygons surrounding each mine (which agree with the planned schedule of underground blasts). Official time is 1–2 h ahead of Universal Time in peninsular Spain, and 0–1 h in peninsular Portugal, depending on daylight saving time. Digital elevation model from Farr et al. (2007)

reliability of identifying and removing blasts in seismic catalogues based only on day/night activity ratios or by their occurrence on working days (instead of weekends).

Identifying blasts from their location alone is hampered by location errors. This is evidenced by the wide dispersion of blast epicentres in the examples shown, especially in Trimouns (Figs. 16 and 17). Quarry or mine blasts have very shallow origin depths ($\sim$ 0 km), what might help in distinguishing them from natural (deeper) earthquakes. But these small events, typically recorded by few stations, have poor depth determinations. In the three examples detailed here, most blasts have no depth determined independently (depth is fixed to 0 km in the analysis), and those for which depth is calculated have diverse reported depths, even $\geq$ 10 km in several cases, evidencing poor depth accuracy.

For statistical analysis of the catalogue, it is useful to set a magnitude threshold above which blasts are absent or highly unlikely (e.g. Habermann 1987). In Europe, quarry blasts do not usually reach $M \sim 2.5$ (Giardini et al. 2004; Gulia 2010). But in Spain, blasts recorded and identified by IGN occasionally reach $m_{bLg} > 3.0$ (Rueda Núñez 2006). An exceptional case of mining-related seismicity in Spain was the ground shaking caused by the collapse of the Reocín mine (7 January 1965), which reached $m_{bLg} = 4.1$ and whose entry was recently removed from the IGN catalogue. This early exception aside, it seems likely that only small collapse events may be confused with natural seismicity and included in the catalogue, such as a probable case with $m_{bLg} = 2.2$ analysed by Alvarez-Garcia et al. (2013).

To estimate the upper magnitude threshold of non-tectonic events contaminating the IGN catalogue, I compared it with the list of non-tectonic events in the same region, supplied by the EMSC for January 1998–July 2012 (Gilles Mazet-Roux, pers. comm., 2015). The list contains over 34,000 events, mostly mine explosions, and is built with data contributions from IGN and other agencies, plus further screening by EMSC operators, which considers the location of known blasting sites and the times at which blasts are typically detonated (Godey et al. 2013). I considered that an event in the IGN catalogue was also on the EMSC list if there was a difference in origin time $\leq$ 1.5 s and epicentral distance $\leq$ 10 km between them. This lead to identifying 210 non-tectonic events

in the IGN catalogue, all located in the Iberian Peninsula and southern France (none in Northern Africa or the Canary Islands). This figure is optimistic, considering the number of potential blasts already identified in the cases analysed here. However, it is expected to include at least the largest blasts, which should be the easiest to identify and the most consistently located in both catalogues. The IGN magnitudes of these events was $m_{bLg} \leq 2.5$ and in most cases ≤ 2.0. Is thus unlikely that the IGN catalogue is contaminated by non-tectonic events with $m_{bLg} \gtrsim 2.5$, an observation that also holds for the blasts identified in the examples above and for the collapse event discussed by Alvarez-Garcia et al. (2013).

8 Concluding remarks

This paper has tried to offer a comprehensive review of the Spanish National Earthquake Catalogue and its main overall properties, focusing on the instrumental era. The evolution of the catalogue is detailed, highlighting the upgrades of the monitoring network, of the techniques used for locating earthquakes and of the determination of magnitudes. These developments have resulted in an heterogeneous catalogue with a marked overall improvement over time.

The hypocentral location precision has improved over the decades and shows a clear spatial pattern, being typically much better in the Iberian Peninsula than elsewhere, especially for the hypocentral depth. The most notable improvement began with the introduction of the new automatic location procedures in November 1997. As in other instances (e.g. Amato and Mele 2008; Custódio et al. 2015), earthquakes in distant offshore areas are the least precisely located, because they are far from the stations and recorded with a large azimuthal gap. The determination of focal mechanisms off the Iberian Peninsula shore also suffers from these factors (Domingues et al. 2013). Such limitations are particulary relevant because tsunamis and the largest earthquakes in the region have indeed originated in such areas. Ocean-bottom seismometers could greatly improve offshore monitoring, as highlighted by results from temporary deployments (e.g. Geissler et al. 2010) and theoretical modelling (Zahradník and Custódio 2012). Further improvements are expected from the use of refined velocity models (e.g. Lozano et al. 2016).

The catalogue includes a temporal and spatial mixture of non-equivalent magnitude scales. In other catalogues such diversity is known to affect, e.g. the calculated seismicity rates and b-values, and should be carefully considered before any statistical analysis (e.g. Habermann 1987; Zúñiga and Wiemer 1999; Tormann et al. 2010, and references therein). Homogenizing the magnitudes from this catalogue has been carried out in several instances by converting them all into moment magnitude by using empirical relations (Mezcua et al. 2011; Martínez Solares et al. 2013; Gaspar-Escribano et al. 2016, and references therein). But reliable conversion relationships (Cabañas et al. 2015) are only available for magnitudes $\gtrsim 3$ (i.e. for a minority of events), since original moment magnitudes for small earthquakes in the area can rarely be calculated. Backward review of catalogue magnitudes into a single scale when possible (e.g. Tormann et al. 2010) would alleviate part of this heterogeneity.

Improvements in earthquake detection have enabled recording increasing numbers of earthquakes in the region per unit time, evidencing a progressive lowering of the magnitude of completeness, M_c. For the first time for this catalogue, detailed maps of M_c are here calculated, during several periods in each region analysed. These periods, as short as data availability allows, are chosen considering the reviewed evolution of the catalogue, taking care that during each of them the network was relatively stable, and the same routines for location and magnitude determination were used. This kind of detailed temporal analysis had so far only been carried out for catalogues with many more events (e.g. Hutton et al. 2010). The appropriateness of the temporal and spatial choices of the analysis is evidenced by the consistency of the results (the lowest M_c is systematically found in the areas with densest monitoring) and their typically low uncertainties (except for areas where earthquakes with different magnitude scales overlap). M_c first improved slowly from the 1960s to the 1990s. A sudden improvement was due to the introduction of new automatic location routines in late 1997, and a dramatic one was achieved by the new digital, broadband network from 2002 onwards. The catalogue is more complete in the most seismically active (better monitored) areas within the Iberian Peninsula and the Canary Islands than elsewhere, although a progressive improvement of completeness over the years is observed even in offshore areas.

A weekend effect (more earthquakes recorded during weekends) is found in the catalogue for the first time, as well as the better known daily variations (more earthquakes recorded during nighttime). Both effects are interpreted as related to the variable amplitudes of artificial noise. They disappear when only the complete part of the catalogue is regarded, which supports the values of magnitude of completeness calculated here.

Clear examples of contamination by quarry and mine blasts (with magnitudes $\lesssim 2.5$) are pinpointed, despite the monitoring agency has successfully removed the vast majority of artificial explosions from the catalogue. The cases studied here indicate that useful complementary screening would be provided by checking known mining sites and their typical blasting schedule. Examples of large-scale underground mines are found where blasts are set off during nights and weekends, indicating that it is not always correct to assume that blasts are only made during daylight times (e.g. Wiemer and Baer 2000) and in weekdays.

Hopefully, this review will provide useful guidelines for users of this valuable database and also insight for planning where and how this catalogue would most benefit from future upgrades in instrumentation or in routine analysis of the seismic data.

References

Aki K (1965) Maximum likelihood estimate of b in the formula $\log N = a - bM$ and its confidence limits. Bull Earthq Res Inst Univ Tokyo 43:237–239

Alguacil G, Martín Dávila J (2003) Stations and seismological networks in the Iberian Peninsula: state of the art. Fís Tierra 15:29–48

Almendros J, Ibáñez JM, Alguacil G et al (2000) A double seismic antenna experiment at Teide Volcano: existence of local seismicity and lack of evidences of volcanic tremor. J Volcanol Geotherm Res 103:439–462

Almendros J, Ibáñez JM, Carmona E, Zandomeneghi D (2007) Array analyses of volcanic earthquakes and tremor recorded at Las Cañadas caldera (Tenerife Island, Spain) during the 2004 seismic activation of Teide volcano. J Volcanol Geotherm Res 160:285–299

Alvarez-Garcia IN, Ramos-Lopez FL, Gonzalez-Nicieza C, Alvarez-Fernandez MI, Alvarez-Vigil AE (2013) The mine collapse at Lo Tacón (Murcia, Spain), possible cause of the Torre Pacheco earthquake (2nd May 1998, SE Spain). Eng Fail Anal 28:115–133

Amante C, Eakins BW (2009) ETOPO1 1 arc-minute global relief model: procedures, data sources and analysis. NOAA Technical Memorandum NESDIS NGDC-24

Amato A, Mele FM (2008) Performance of the INGV National Seismic Network from 1997 to 2007. Ann Geophys 51:417–431

Ammon CJ, Lay T, Simpson DW (2010) Great earthquakes and global seismic networks. Seismol Res Lett 81:965–971

Anduaga A (2004) Earthquakes, damage, and prediction: the Spanish seismological Service, 1898–1930. Earth Sci Hist 23:175–207

Anduaga A (2009) Geofísica, economía y sociedad en la España contemporánea. Consejo Superior de Investigaciones Científicas, Madrid

Atef AH, Liu KH, Gao SS (2009) Apparent weekly and daily earthquake periodicities in the western United States. Bull Seism Soc Am 99:2273–2279

Ayadi A, Bezzeghoud M (2015) Seismicity of Algeria from 1365 to 2013: maximum observed intensity map (MOI_{2014}). Seismol Res Lett 86:236–244

Badal J, Samardjieva E, Payo G (2000) Moment magnitudes for early (1923–1961) instrumental Iberian earthquakes. Bull Seism Soc Am 90:1161–1173

Bahavar M, North R (2002) Estimation of background noise for International Monitoring System seismic stations. Pure Appl Geophys 159:911–944

Båth M (compiler, 1969) Handbook on earthquake magnitude determinations, 2nd edn, VESIAC Special Report, Geophysics Laboratory, Willow Run Laboratories, University of Michigan

Båth M (1981) Earthquake magnitude - recent research and current trends. Earth Sci Rev 17:315–398

Batlló J (2004) Catálogo inventario de sismógrafos antiguos españoles [A Catalogue of Old Spanish Seismographs]. Instituto Geográfico Nacional, Madrid

Batlló J, Bormann P (2000) A catalog of old Spanish seismographs. Seismol Res Lett 71:570–582

Batlló J, Stich D, Palombo B, Macia R, Morales J (2008) The 1951 M_w 5.2 and M_w 5.3 Jaén, Southern Spain, earthquake doublet revisited. Bull Seism Soc Am 98:1535–1545

Benson R, Lindholm CD, Ludwin R, Qamar A (1992) A method for identifying explosions contaminating earthquake catalogs: application to the Washington Regional Earthquake Catalog. Seismol. Res Lett 63:533–539

Bezada MJ, Humphreys ED (2012) Contrasting rupture processes during the April 11, 2010 deep-focus earthquake beneath Granada, Spain. Earth Planet Sci Lett 353–354:38–46

Biegalski KF, Bohlin J, Carter JA, Coyne J, Dompierre D, Novosel G, Rinehart C (1999) Formats and protocols for messages – IMS1.0. International Data Center, Document SAIC-99/3004

Bonnefoy-Claudet S, Cotton F, Bard PY (2006) The nature of noise wavefield and its applications for site effects studies. A literature review. Earth Sci Rev 79:205–227

Boyd TM, Snoke JA (1984) Error estimates in some commonly used earthquake location programs. Earthq Not 55:3–6

Bratt SR, Bache TC (1988) Locating events with a sparse network of regional arrays. Bull Seism Soc Am 78:780–798

Buforn E, Coca P, Udías A, Lasa C (1997) Source mechanism of intermediate and deep earthquakes in southern Spain. J Seismol 1:113–130

Buforn E, Pro C, Cesca S, Udías A, del Fresno C (2011) The 2010 Granada, Spain, deep earthquake. Bull Seism Soc Am 101:2418–2430

Cabañas L, Alcalde JM, Carreño E, Bravo JB (2014) Characteristics of observed strong motion accelerograms from the 2011 Lorca (Spain) earthquake. Bull Earthq Eng 12:1909–1932

Cabañas L, Rivas-Medina A, Martínez-Solares JM, Gaspar-Escribano JM, Benito B, Antón R, Ruiz-Barajas S (2015) Relationships between M_w and other earthquake size parameters in the Spanish IGN seismic catalog. Pure Appl Geophys 172:2397–2410

Calvert A, Sandvol E, Seber D, Barazangi M, Vidal F, Alguacil G, Jabour N (2000) Propagation of regional seismic phases (Lg and Sn) and Pn velocity structure along the Africa–Iberia plate boundary zone: tectonic implications. Geophys J Int 142:384–408

Canas Torres JA, Vidal Sánchez F (2001) La nueva red sísmica nacional. In: Capote del Villar R, Martínez Díaz JJ (eds) El Riesgo Sísmico, Prevención y Seguro. Consorcio de Compensación de Seguros, Madrid (Spain), pp 147–162

Carniel R, Tárraga M, Barazza F, García A (2008) Possible interaction between tectonic events and seismic noise at Las Cañadas Volcanic Caldera, Tenerife, Spain. Bull Volcanol 70:1113–1121

Carreño E (1999) Instituto Geográfico Nacional (IGN), Madrid, Spain. CSEM-EMSC Newslet 15:10–11

Carreño E, Galán J, Sánchez M (1991a) Microseismicity studies in Southern Spain. In: Mezcua J, Udías A (eds) Seismicity, seismotectonics and seismic risk of the Ibero-Maghrebian region. Monografía 8, Instituto Geográfico Nacional, Madrid, Spain, pp 79–86

Carreño E, Rueda J, López Casado C, Galán J, Peláez JA (1991b) Spanish national strong motion network. Recording of the Huelva earthquake of 20 December, 1989. Pure Appl Geophys 136:395–404

Carreño E, López C, Bravo B, Expósito P, Gurría E, García O (2003) Seismicity of the Iberian Peninsula in the instrumental period: 1985-2002. Fís Tierra 15:73–91

Carreño E, López C, Villamayor A, Gracia F, Alonso A, Ruiz E (2001) Estación sísmica de Sonseca. Descripción general. In: Capote del Villar R, Martínez Díaz JJ (eds) El Riesgo

Sísmico, Prevención y Seguro. Consorcio de Compensación de Seguros, Madrid (Spain), pp 163–177

Carreño Herrero E, Valero Zornoza JF (2011) The Iberian Peninsula seismicity for the instrumental period: 1985-2011. Enseñ Cienc Tierra 19:289–295

Carrilho FJR, Nunes JAC, Pena JOA, Senos ML (2004) Catálogo Sísmico de Portugal Continental e Região Adjacente para o Período 1970–2000. Instituto de Meteorologia, Lisbon

Cattaneo M, Caffagni E, Carannante S, D'Alema E, Frapiccini M, Ladina C, Marzorati S, Monachesi G (2014) A catalogue of non-tectonic earthquakes in central-eastern Italy. Ann Geophys 57:S0328

Cesca S, Grigoli F, Heimann S, González Á, Buforn E, Maghsoudi S, Blanch E (2013) September–October seismic sequence offshore Spain: a case of seismicity triggered by gas injection? Geophys J Int 198:941–953

Chadwick J (2007) The riches of Neves-Corvo and Aljustrel. Int Mining January:42–51

Chazalon A, Campillo M, Gibson R, Carreno E (1993) Crustal wave propagation anomaly across the Pyrenean Range. Comparison between observations and numerical simulations. Geophys J Int 115:829–838

Chevrot S, Sylvander M, Delouis B (2011) A preliminary catalog of moment tensors for the Pyrenees. Tectonophysics 510:239–251

Custódio S, Batlló J, Martins D et al (2012) Station COI: dusting off an old seismic station. Seismol Res Lett 83:863–869

Custódio S, Dias NA, Caldeira B et al (2014) Ambient noise recorded by a dense broadband seismic deployment in Western Iberia. Bull Seism Soc Am 104:2985–3007

Custódio S, Dias NA, Carrilho F et al (2015) Earthquakes in western Iberia: improving the understanding of lithospheric deformation in a slowly deforming region. Geophys J Int 203:127–145

D'Alessandro A, Badal J, D'Anna G, Papanastassiou D, Baskoutas I, Özel NM (2013) Location performance and detection threshold of the Spanish national seismic network. Pure Appl Geophys 170:1859–1880

Dañobeitia JJ (1980) Interpretación de la estructura de la corteza en el Archipiélago Canario a partir de perfiles sísmicos profundos de refracción. Ph.D Thesis, Universidad Complutense de Madrid

Del Pin E, Carniel R, Tárraga M (2008) Event recognition by detrended fluctuation analysis: an application to Teide-Pico Viejo volcanic complex, Tenerife, Spain. Chaos Soliton Fractal 36:1173–1180

de Parseval P, Fontan F, Martin F, Freeet J, Jiang SY, Wang RC (2004) Geology and ore genesis of the Trimouns talc-chlorite ore deposit, Pyrenees, France. Acta Petrol Sinica 20:877–886

Díaz J, Villaseñor A, Morales J et al (2010) Background noise characteristics at the IberArray broadband seismic network. Bull Seism Soc Am 100:618–628

Domingues A, Custódio S, Cesca S (2013) Waveform inversion of small-to-moderate earthquakes located offshore southwest Iberia. Geophys J Int 192:248–259

Domínguez Cerdeña I, del Fresno C, Rivera L (2011) New insight on the increasing seismicity during Tenerife's 2004 volcanic reactivation. J Volcanol Geotherm Res 206:15–29

Domínguez Cerdeña I, del Fresno C, Gomis Moreno A (2014) Seismicity patterns prior to the 2011 El Hierro eruption. Bull Seism Soc Am 104:567–575

Dowla FU (1996) Calibration of the Sonseca Array with Large Magnitude Regional and Teleseismic Events. Report UCRL-ID-125023. Lawrence Livermore National Laboratory, Livermore, California

Dreger DS, Helmberger DV (1993) Determination of source parameters at regional distances with three-component sparse network data. J Geophys Res 98:8107–8125

Durá-Gómez I, Talwani P (2010) Reservoir-induced seismicity associated with the Itoiz Reservoir, Spain: a case study. Geophys J Int 181:343–356

Efron B (1979) Bootstrap methods: another look at the jackknife. Ann Stat 7:1–26

Euroseismos Project (2006) Index of bulletins of Spain, Istituto Nazionale di Geofisica e Vulcanologia, storing.ingv.it/bulletins/Spain/index.html

Farr TG, Rosen PA, Caro E et al (2007) The shuttle radar topography mission. Rev Geophys 45:RG2004

Fréchet J, Rivera L (2012) Horizontal pendulum development and the legacy of Ernst von Rebeur-Paschwitz. J Seismol 16:315–343

Frohlich C (2006) Deep earthquakes. Cambridge University Press, Cambridge

García A, Fernández-Ros A, Berrocoso M, Marrero JM, Prates G, De la Cruz-Reyna S, Ortiz R (2014) Magma displacements under insular volcanic fields, applications to eruption forecasting: El Hierro, Canary Islands, 2011–2013. Geophys J Int 197:322–334

García Fernández M (1986) Relative location accuracy of the Spanish seismic network for earthquakes in the Iberian region. Revista Geofis 42:3–8

García Fernández M, Kijko A, López Arroyo A (1987) The new Spanish seismic network: optimization and location capability. In: Mayer-Rosa D, van Gils JM, Stiller H (eds) European seismological commission: activity reports 1984-1986 and Proceedings of the XX general assembly 1986 in Kiel, pp 88–102. Publication series of the Swiss Seismological Service, No. 101. Federal Institute of Technology, Zürich

García Fernández M, Kijko A, Carracedo JC, Soler V (1988) Optimum station distribution to monitor seismic activity of Teide volcano, Tenerife, Canary Islands. J Volcanol Geotherm Res 35:195–204

García Maneiro CH, Maqueda Jiménez S, Pazos Pérez L, Carnero Ortiz F (2012) Voladuras de cámara de la mina de Aguas Teñidas. Industria y Minería 390:25–31

García-Mayordomo J, Insua-Arévalo JM, Martínez-Díaz JJ et al (2012) The quaternary active faults database of Iberia (QAFI v.2.0). J Iber Geol 38:285–302

García Vargas M, Rueda J, García Blanco RM, Mezcua J (2016) A real-time discrimination system of earthquakes and explosions for the mainland Spanish seismic network. Pure Appl Geophys. doi:10.1007/s00024-016-1330-z

Gaspar-Escribano JM, Rivas-Medina A, Parra H, Cabañas L, Benito B, Ruiz Barajas S, Martínez Solares JM (2016) Uncertainty assessment for the seismic hazard map of Spain. Eng Geol 199:62–73

Geissler WH, Matias L, Stich D et al (2010) Focal mechanisms for sub-crustal earthquakes in the Gulf of Cadiz from a dense OBS deployment. Geophys Res Lett 37:L18309

Gentili S, Sugan M, Peruzza L, Schorlemmer D (2011) Probabilistic completeness assessment of the past 30 years of seismic monitoring in northeastern Italy. Phys Earth Planet Inter 186:81–96

Giardini D, Wiemer S, Fäh D, Deichmann D (2004) Seismic hazard assessment of Switzerland, 2004. Report, Swiss Seismological Service, ETH Zurich

Godey S, Bossu R, Guilbert J, Mazet-Roux G (2006) The Euro-Mediterranean Bulletin: a comprehensive seismological bulletin at regional scale. Seismol Res Lett 77:460–474

Godey S, Bossu R, Guilbert J (2013) Improving the Mediterranean seismicity picture thanks to international collaborations. Phys Earth Planet Inter 63:3–11

González de Vallejo LI, García-Mayordomo J, Insua JM (2006) Probabilistic seismic-hazard assessment of the Canary Islands. Bull Seism Soc Am 96:2040–2049

Grünthal G, Wahlström R (2012) The European-Mediterranean Earthquake Catalogue (EMEC) for the last millennium. J Seismol 16:535–570

Gulia L (2010) Detection of quarry and mine blast contamination in European regional catalogues. Nat Hazards 53:229–249

Gulia L, Wiemer S, Wyss M (2012) Catalog artifacts and quality control. Community online resource for statistical seismicity analysis doi:10.5078/corssa-93722864. Available at www.corssa.org

Gutenberg B, Richter CF (1944) Frequency of earthquakes in California. Bull Seism Soc Am 34:185–188

Habermann RE (1987) Man-made changes of seismicity rates. Bull Seism Soc Am 77:141–159

Hamdache M, Peláez JA, Talbi A, López Casado C (2010) A unified catalog of main earthquakes for Northern Algeria from A.D. 856 to 2008. Seismol Res Lett 81:732–739

Hanks TC, Kanamori H (1979) A moment magnitude scale. J Geophys Res 84:2348–2350

Harbi A, Sebaï A, Benmedjber M et al (2015) The Algerian homogenized macroseismic database (267–1989): a deeper insight into the Algerian historical seismicity. Seismol Res Lett 54:725–747

Hasting M, Barrientos S (2002) The upgrade of the International Monitoring System primary station at Sonseca, Spain, (PS-40): A before and after comparison of the short-period array. In: Proceedings of the 24th seismic research review – nuclear explosion monitoring: innovation and integration. Ponte Vedra Beach, Florida (USA), pp 927–939

Havskov J, Ottemöller L (2010) Routine data processing in earthquake seismology. Springer, Dordrecht (Netherlands)

Herraiz M, Lázaro M (1991) Microearthquake distribution in the Granada region. In: Mezcua J, Udías A (eds) Seismicity, seismotectonics and seismic risk of the Ibero-Maghrebian region, pp 65–77. Monografía 8, Instituto Geográfico Nacional, Madrid, Spain

Husen S, Hardebeck JL (2010) Earthquake location accuracy. Community online resource for statistical seismicity analysis, doi:10.5078/corssa-55815573. Available at www.corssa.org

Hutton K, Woessner J, Hauksson E (2010) Earthquake monitoring in Southern California for seventy-seven years (1932–2008). Bull Seism Soc Am 100:423–446

IAG – Instituto Andaluz de Geofísica (2016) Red Sísmica de Andalucía, iagpds.ugr.es/pages/red_sismica

Ibáñez JM, De Angelis S, Díaz-Moreno A, Hernández P, Alguacil G, Posadas A, Pérez N (2012) Insights into the 2011-2012 submarine eruption off the coast of El Hierro (Canary Islands, Spain) from statistical analyses of earthquake activity. Geophys J Int 191:659–670

ICGC – Institut Cartogràfic i Geològic de Catalunya (2016) Seismic network of Catalonia. www.igc.cat/web/en/sismologia_xsis.html

IGN – Instituto Geográfico Nacional (1991) Spanish National Seismic Network. In: Mezcua J, Udías A (eds) Seismicity, seismotectonics and seismic risk of the Ibero-Maghrebian region, pp 3–15. Monografía 8, Instituto Geográfico Nacional, Madrid, Spain

IGN – Instituto Geográfico Nacional (2016a) Servicio de Información Sísmica. www.ign.es/ign/layout/sismo.do

IGN – Instituto Geográfico Nacional (2016b) Vigilancia Volcánica. www.ign.es/ign/layout/volcaVolcanologia.do

ISC – International Seismological Centre (2016a) International Registry of Seismograph Stations, www.isc.ac.uk/registries/, Internatl. Seis. Cent., Thatcham, United Kingdom

ISC – International Seismological Centre (2016b) On-line bulletin. www.isc.ac.uk, Internatl. Seis. Cent., Thatcham, United Kingdom

Ishimoto M, Iida K (1939) Observations sur les séismes enregistrés par le microséismographe construit dernièrement (I). Bull Earthq Res Inst Univ Tokyo 17:443–478. [In Japanese, with French abstract]

Iwata T (2013) Estimation of completeness magnitude considering daily variation in earthquake detection capability. Geophys J Int 194:1909–1919

Jiménez MJ, García-Fernández M (1996) Aftershock sequence of the 9 May 1989 Canary Islands earthquake. Tectonophysics 255:157–162

Kagan YY (2003) Accuracy of modern global earthquake catalogs. Phys Earth Planet Inter 135:173–209

Kværna T, Ringdal F (2013) Detection capability of the seismic network of the International Monitoring System for the comprehensive nuclear-test-ban treaty. Bull Seism Soc Am 103:759–772

Kwiatek G, Plenkers K, Nakatani M, Yabe Y, Dresen G, JAGUARS-Group (2010) Frequency-magnitude characteristics down to magnitude -4.4 for induced seismicity recorded at Mponeng gold mine, South Africa. Bull Seism Soc Am 100:1165–1173

Lee WHK, Lahr JC (1975) HYPO71 (revised): a computer program for determining hypocenter, magnitude, and first motion pattern of local earthquakes. U.S. Geological Survey Open File Report 75-311

Leistel JM, Marcoux E, Thiéblemont D, Quesada C, Sánchez A, Almodóvar GR, Pascual E, Sáez R (1998) The volcanic-hosted massive sulphide deposits of the Iberian Pyrite Belt. Miner Depos 33:2–30

López C (2008) Nuevas fórmulas de magnitud para la Península Ibérica y su entorno. MsC Thesis, Departamento de Física

de la Tierra, Astronomía y Astrofísica I. Universidad Complutense de Madrid (Spain)

López C, Muñoz D (2003) Magnitude formulas in the Spanish bulletins and catalogues. Fís Tierra 15:49–71

López C, Blanco MJ, Abella R et al (2012) Monitoring the volcanic unrest of El Hierro (Canary Islands) before the onset of the 2011–2012 submarine eruption. Geophys Res Lett 39:L13303

López Casado C, Molina S, Giner JJ, Delgado J (2000) Magnitude-intensity relationships in the Ibero-Magrebhian region. Pure Appl Geophys 22:271–297

Lozano L, Cantavella JV, Barco J, Carranza M, Burforn E (2016) 3D crustal seismic velocity model for the Gulf of Cadiz and adjacent areas (SW Iberia margin) based on seismic reflection and refraction profiles. Geophys Res Abstr 18:EGU2016-2544

Luzón F, García-Jerez A, Santoyo MA, Sánchez-Sesma FJ (2010) Numerical modelling of pore pressure variations due to time varying loads using a hybrid technique: the case of the Itoiz reservoir (Northern Spain). Geophys J Int 180:327–338

Mancilla F, Del Pezzo E, Stich D, Morales J, Ibañez J, Bianco F (2012) Q_P and Q_S in the upper mantle beneath the Iberian peninsula from recordings of the very deep Granada earthquake of April 11, 2010. Geophys Res Lett 39:L09303

Martí J, Ortiz R, Gottsmann J, Garcia A, De La Cruz-Reyna S (2009) Characterising unrest during the reawakening of the central volcanic complex on Tenerife, Canary Islands, 2004–2005, and implications for assessing hazards and risk mitigation. J Volcanol Geotherm Res 182:23–33

Martín R, Stich D, Morales J, Mancilla F (2015) Moment tensor solutions for the Iberian-Maghreb region during the Iber-Array deployment (2009–2013). Tectonophysics 663:261–274

Martín Dávila J, Gárate Pasquín J, Pazos García A, Catalán Morollón M (2006) The Geophysics in the Royal Naval Institute and Observatory in San Fernando. Fís Tierra 18:119–135

Martínez-Díaz JJ, Bejar-Pizarro M, Álvarez-Gómez JA, Mancilla FL, Stich D, Herrera G, Morales J (2012) Tectonic and seismic implications of an intersegment rupture: The damaging May 11th 2011 Mw 5.2 Lorca, Spain, earthquake. Tectonophysics 546–547:28–37

Martínez Solares JM (1981) El terremoto de Andalucía del 25 de diciembre de 1884. Instituto Geográfico Nacional, Madrid, Spain

Martínez Solares JM (1992) Optimización de parámetros de localización para distintos tipos de redes sísmicas. Aplicación a la Península Ibérica. PhD Thesis, Universidad Complutense de Madrid

Martínez Solares JM (1995) Métodos de localización epicentral mediante el procesamiento de señales de dispositivos sísmicos. In: Mezcua J (ed) Redes sísmicas regionales, pp 113–144. Monografía 11, Instituto Geográfico Nacional, Madrid (Spain)

Martínez Solares JM (2003) Historical seismicity of the Iberian Peninsula. Fis Tierra 15:13–28

Martínez Solares JM, López Arroyo A (2004) The great historical 1755 earthquake. Effects and damage in Spain. J Seismol 8:275–294

Martínez Solares JM, Mezcua J (2002) Catálogo Sísmico de la Península Ibérica (880 a.C. – 1900). Monografía 18, Instituto Geográfico Nacional, Madrid (Spain)

Martínez Solares JM, Cabañas Rodríguez L, Benito Oterino MB, Rivas Medina A, Gaspar Escribano JM, Ruíz Barajas S, Rodríguez Zaloña Ó (2013) Actualización de mapas de peligrosidad sísmica de España 2012. Instituto Geográfico Nacional, Madrid, Spain

McNamara DE, Walter WR (2001) Mapping crustal heterogeneity using Lg propagation efficiency throughout the Middle East, Mediterranean, Southern Europe and Northern Africa. Pure Appl Geophys 158:1165–1188

Mezcua J (1995) Fundamentos de la red sísmica de España. In: Mezcua J (ed) Redes sísmicas regionales, pp 63–86. Monografía 11, Instituto Geográfico Nacional, Madrid (Spain)

Mezcua J, Martínez Solares JM (1983) Sismicidad del Área Ibero-Mogrebí. Instituto Geográfico Nacional, Madrid (Spain). Publicación Técnica 203

Mezcua J, Rueda J (1994) Earthquake relative location based on waveform similarity. Tectonophysics 233:253–263

Mezcua J, Buforn E, Udías A, Rueda J (1992) Seismotectonics of the Canary Islands. Tectonophysics 208:447–452

Mezcua J, Rueda J, García Blanco RM (2004) Reevaluation of historic earthquakes in Spain. Seismol Res Lett 75:75–81

Mezcua J, García Blanco RM, Rueda J (2008) On the strong ground motion attenuation in Spain. Bull Seism Soc Am 98:1343–1353

Mezcua J, Rueda J, García Blanco RM (2011) A new probabilistic seismic hazard study of Spain. Nat Hazards 59:1087–1108

Mezcua J, Rueda J, García Blanco RM (2013) Iberian Peninsula historical seismicity revisited: an intensity data bank. Seismol Res Lett 84:9–18

Michael AJ (2014) How complete is the ISC-GEM global earthquake catalog? Bull Seism Soc Am 104:1829–1837

Michelini A, De Simoni B, Amato A, Boschi E (2005) Collecting, digitizing, and distributing historical seismological data. Eos Trans Am Geophys Union 86:261–266

Mignan A (2012) Functional shape of the earthquake frequency-magnitude distribution and completeness magnitude. J Geophys Res 117:B08302

Mignan A, Woessner J (2012) Estimating the magnitude of completeness for earthquake catalogs. Community Online Resource for Statistical Seismicity Analysis. doi:10.5078/corssa-00180805. Available at www.corssa.org

Morales J, Cantavella JV, Mancilla FL et al (2014) The 2011 Lorca seismic series: temporal evolution, faulting parameters and hypocentral relocation. Bull Earthq Eng 12:1871–1888

Moritz H (2000) Geodetic Reference System 1980. J Geodesy 74:128–133

Mouayn I (2007) The M_D scale in northern Morocco: a comparative study of two empirical approaches. Pure Appl Geophys 164:957–974

Mouayn I, Tadili BA, Brahim LA, Ramdani M, Limouri M, Jabour N (2004) Duration magnitude scale and site residuals for northern Morocco. Pure Appl Geophys 161:1061–1080

Muñoz D, Udías A (1982) Historical development of Spain's catalogs of earthquakes. Bull Seism Soc Am 72:1039–1042

Nagy W (1996) New region-dependent travel-time handling facilities at the IDC; functionality, testing and implementation details. Science Applications International Corporation Technical Report, SAIC-96/1179

Nanjo KZ, Ishibe T, Tsuruoka H, Schorlemmer D, Ishigaki Y, Hirata N (2010) Analysis of the completeness magnitude and seismic network coverage of Japan. Bull Seism Soc Am 100:3261–3268

NIMA – National Imaging and Mapping Agency (2000) Department of Defense World Geodetic System 1984. Its definition and relationships with local geodetic systems. NIMA Technical Report 8350.2, 3rd edn. St. Louis (Missouri USA)

Noriega R, Ugalde A, Villaseñor A, Jurado MJ (2015) Spatial variation of Lg-wave attenuation in the Iberian Peninsula. Bull Seism Soc Am 105:420–430

Nuttli OW (1973) Seismic-wave attenuation and magnitude relations for eastern North-America. J Geophys Res 78:876–885

Panzera F, Zechar JD, Vogfjörd KS, Eberhard DAJ (2016) A revised earthquake catalogue for south Iceland. Pure Appl Geophys 173:97–116

Payo Subiza G, Gómez-Menor R (1998) Historia del Observatorio Geofísico de Toledo. Instituto Geográfico Nacional, Madrid

Peláez JA, Chourak M, Tadili BA, Aït Brahim L, Hamdache M, López Casado C, Martínez Solares JM (2007) A catalog of main Moroccan earthquakes from 1045 to 2005. Seismol Res Lett 78:614–621

Peláez JA, Hamdache M, Martínez Solares JM (2012) Relationship between computed mb (IGN) and ML (CRAAG) magnitudes for earthquakes located in Northern Algeria. In: Proceedings, 7ª Asamblea Hispano Portuguesa de Geodesia y Geofísica. San Sebastián, pp 189–192

Pena JOA, Nunes JAC, Carrilho FJR (2014) Catálogo Sísmico de Portugal Continental e Região Adjacente para o Período 1961–1969. Instituto Português do Mar e da Atmosfera. Lisbon

Peterson J, Hutt CR (2014) World-Wide Standardized Seismograph Network: a data users guide, U.S. Geological Survey open-file report 2014-1218, Reston

Posadas AM, Vidal F, de Miguel F, Alguacil G, Peña J, Ibañez JM, Morales J (1993) Spatial-temporal analysis of a seismic series using the principal components method: the Antequera series, Spain, 1989. J Geophys Res 98:1923–1932

Roberts NS, Bell AF, Main IG (2015) Are volcanic seismic b-values high, and if so when? J Volcanol Geotherm Res 308:127–141

Roca A., Izquierdo A, Sousa-Oliveira C, Martínez-Solares JM (2004) An outline of earthquake catalogues, databases and studies of historical seismicity in the Iberian Peninsula. Ann Geophys 47:561–570

Roca A, Locati M, Susagna T et al (2011) Archivo online de datos macrosísmicos de la Península Ibérica. In: Actas del Cuarto congreso nacional de ingeniería sísmica. Granada (Spain). www.earth-prints.org/handle/2122/8599

Rodríguez de la Torre F (1989) Management and interpretation of hemerographical sources concerning research about historical Iberian seismicity. In: Proceedings of the workshop on historical earthquakes in the Ibero-Maghrebian region. Methodological approach and case studies, vol IV. Lisbon, pp 23–94

Rodríguez de la Torre F (2004) Iberian seismic catalogue. A complete revision of all the 19th century. In: Papers of the European Seismological Commission general assembly, Potsdam. Paper SCA-3, www.esc-web.org/the-esc-general-assembly/111-esc-papers-september-2004.html

Rosa CJP, McPhie J, Relvas JMRS (2010) Type of volcanoes hosting the massive sulfide deposits of the Iberian Pyrite Belt. J Volcanol Geotherm Res 194:107–126

Rost S, Thomas C (2002) Array seismology: methods and applications. Rev Geophys 40:1008

Rueda J (1995) Análisis y procesamiento de datos en la Red Sísmica Nacional. In: Mezcua J (ed) Redes sísmicas regionales, pp 87–112. Monografía 11, Instituto Geográfico Nacional, Madrid (Spain)

Rueda J (2010) Diseño de la alerta (sísmica) IGN. In: Jornada técnica sobre riesgo y peligrosidad de tsunamis en España. Proyectos sobre su predicción y sistemas de alerta. Dirección General de Protección Civil y Emergencias, Rivas de Vaciamadrid, Spain, September 10, www.proteccioncivil.org/catalogo/naturales/jornada-riesgo-tsunamis/presentaciones/index.htm

Rueda Núñez JJ (2006) Discriminación sísmica mediante el análisis de las señales generadas por explosiones y terremotos. Aplicación a la región suroeste de Europa-Norte de África. PhD Thesis, Universidad Politécnica de Madrid (Spain)

Rueda J, Mezcua J (2002) Estudio del terremoto del 23 de septiembre de 2001 en Pego (Alicante). Obtención de una relación $mbLg - M_w$ para la Península Ibérica. Rev Soc Geol Esp 15:159–173

Rueda J, Mezcua J (2005) Near-real-time seismic moment-tensor determination in Spain. Seismol Res Lett 76:455–465

Rueda J, Mezcua J (2006) Seismic network LOcation CApability program, LOCA 1.0, www.fundaciongarciasineriz.es/descargas/loca.zip

Rueda J, Mezcua J (2015) Orientation analysis of the Spanish broadband national network using Rayleigh-wave polarization. Seismol Res Lett 86:929–940

Ruiz M, Gaspà O, Gallart J, Díaz J, Pulgar JA, García-Sansegundo J, López-Fernández C, González-Cortina JM (2006) Aftershocks series monitoring of the September 18, 2004 M=4.6 earthquake at the western Pyrenees: a case of reservoir-triggered seismicity? Tectonophysics 426:223–243

Rydelek PA, Sacks IS (1989) Testing the completeness of earthquake catalogues and the hypothesis of self-similarity. Nature 337:251–253

Samardjieva E, Payo G, Badal J (1997) Catalogue of Digital Historical Seismograms (1912-1962), Wiechert Seismograph, Geophysical Observatory of Toledo, Instituto Geográfico Nacional, Madrid

Samardjieva E, Payo G, Badal J, López C (1998) Creation of a digital database for XXth century historical earthquakes

occurred in the Iberian area. Pure Appl Geophys 152:139–163

Samardjieva E, Payo G, Badal J (1999) Magnitude formulae and intensity-magnitude relations for early instrumental earthquakes in the Iberian Region. Nat Hazards 19:189–204

Sandri L, Marzocchi W (2007) A technical note on the bias in the estimation of the *b*-value and its uncertainty through the least squares technique. Ann Geophys 50:329–339

Santoyo MA, García-Jerez A, Luzón F (2010) A subsurface stress analysis and its possible relation with seismicity near the Itoiz Reservoir, Navarra, Northern Spain. Tectonophysics 482:205–215

Scarpa R, Patanè G, Lombardo G (1983) Space-time evolution of seismic activity at Mount Etna during 1974–1982. Ann Geophys 1:451–462

Schorlemmer D, Woessner J (2008) Probability of detecting an earthquake. Bull Seism Soc Am 98:2103–2117

Schorlemmer D, Wiemer S, Wyss M (2005) Variations in earthquake-size distribution across different stress regimes. Nature 437:539–542

Schorlemmer D, Mele F, Marzocchi W (2010) A completeness analysis of the national seismic network of Italy. J Geophys Res 115:B04308

Schweitzer J, Fyen J, Mykkeltveit S, Kværna T (2009) Seismic arrays. In: Bormann P (ed) New Manual of Seismological Observatory Practice (NMSOP-1), IASPEI. GFZ German Research Center for Geosciences, Potsdam

Secanell R, Bertil D, Martin C et al (2008) Probabilistic seismic hazard assessment of the Pyrenean region. J Seismol 12:323–341

Sens-Schönfelder C, Margerin L, Campillo M (2009) Laterally heterogeneous scattering explains Lg blockage in the Pyrenees. J Geophys Res 114:B07309

Servicio Sismológico (1923) Las informaciones macrosísmicas, Folleto de vulgarización para que sirva de guía a los observadores de temblores de tierra e instrucciones para contestar a los cuestionarios. Talleres del Instituto Geográfico, Madrid

Silva PG, Rodríguez-Pascua MA, Giner Robles JL et al (2014) Catálogo de los efectos geológicos de los terremotos en España. Instituto Geológico y Minero de España and Asociación Española para el Estudio del Cuaternario, Madrid

Souriau A, Pauchet H (1998) A new synthesis of Pyrenean seismicity and its tectonic implications. Tectonophysics 290:221–244

Souriau A, Rigo A, Sylvander M, Benahmed S, Grimaud F (2014) Seismicity in central-western Pyrenees (France): a consequence of the subsidence of dense exhumed bodies. Tectonophysics 621:123–131

Stepp JC (1972) Analysis of completeness in the earthquake sample in the Puget Sound area and its effect on statistical estimates of seismic hazard. In: Procceedings of the International Conference on Microzonation for Safer Construction Research and Applications, vol 2. Seattle, pp 1897–1910

Stich D, Martín R, Morales J (2010) Moment tensor inversion for Iberia-Maghreb earthquakes 2005–2008. Tectonophysics 483:390–398

Storchak DA, Schweitzer J, Bormann P (2003) The IASPEI standard seismic phase list. Seismol Res Lett 74:761–772

Storchak DA, Di Giacomo D, Bondár I, Engdahl ER, Harris J, Lee WHK, Villaseñor A, Bormann P (2013) Public release of the ISC-GEM global instrumental earthquake catalogue (1900-2009). Seismol Res Lett 84:810–815

Susagna T, Goula X (1999) Atles sísmic de Catalunya. Volum 1: Catàleg de sismicitat. Institut Cartogràfic de Catalunya, Barcelona. www.igc.cat/web/files/atles_sismic.pdf

Telesca L, Lovallo M, Lopez C, Marti Molist J (2016) Multiparametric statistical investigation of seismicity occurred at El Hierro (Canary Islands) from 2011 to 2014. Tectonophysics 672–673:121–128

Torcal F, Serrano I, Havskov J, Utrillas JL, Valero J (2005) Induced seismicity around the Tous New Dam (Spain). Geophys J Int 160:144–160

Tormann T, Wiemer S, Hauksson E (2010) Changes of reporting rates in the Southern California earthquake catalog, introduced by a new definition of M_L. Bull Seism Soc Am 100:1733–1742

Udías A (2013) Development of seismology in Spain in the context of the three large earthquakes of 1755, 1884 and, 1954. Earth Sci Hist 32:186–203

Udías A (2015) Historical earthquakes (before 1755) of the Iberian Peninsula in early catalogs. Seismol Res Lett 86:999–1005

Udías A, Stauder W (1996) The Jesuit contribution to seismology. Seismol Res Lett 67(3):10–19 and issue cover figure

Utsu T (1965) A method for determining the value of *b* in a formula $\log n = a - bM$ showing the magnitude-frequency relation for earthquakes. Geophys Bull Hokkaido Univ 13:99–103. [in Japanese, with English abstract]

Veith KF, Clawson GE (1972) Magnitude from short-period P-wave data. Bull Seism Soc Am 62:435–452

Vere-Jones D (1992) Statistical methods for the description and display of earthquake catalogs. In: Walden AT, Guttorp P (eds) Statistics in the environmental and Earth sciences. Edward Arnold, London, pp 220–246

Vila J, Macià R, Correig AM (2005) Spatial variations of local magnitude in earthquakes recorded in northeastern Spain. Pure Appl Geophys 162:515–530

Vinciguerra S, Day S (2013) Magma intrusion as a driving mechanism for the seismic clustering following the 9 May 1989 earthquake swarms at the Canary Islands. Acta Geophys 61:1626–1641

Waldhauser F, Ellsworth WL (2000) A double-difference earthquake location algorithm: Method and application to the northern Hayward fault. Bull Seism Soc Am 90:1353–1368

Wessel P, Smith WHF, Scharroo R, Luis J, Wobbe F (2013) Generic Mapping Tools: improved version released. Eos Trans Am Geophys Union 94:409–410

Wiemer S (2001) A software package to analyze seismicity: ZMAP. Seismol Res Lett 72:374–383

Wiemer S, Baer M (2000) Mapping and removing quarry blast events from seismicity catalogs. Bull Seism Soc Am 90:525–530

Wiemer S, Schorlemmer D (2007) ALM: an asperity-based likelihood model for California. Seismol Res Lett 78:134–140

Wiemer S, Wyss M (2000) Minimum magnitude of completeness in earthquake catalogs: examples from Alaska, the western United States, and Japan. Bull Seism Soc Am 90:859–869

Willemann RJ, Storchak DA (2001) Data collection at the International Seismological Centre. Seismol Res Lett 72:440–453

Woessner J, Wiemer S (2005) Assessing the quality of earthquake catalogues: estimating the magnitude of completeness and its uncertainty. Bull Seism Soc Am 95:684–698

Wyss M, Hasegawa A, Wiemer S, Umino N (1999) Quantitative mapping of precursory seismic quiescence before the 1989, M 7.1 off-Sanriku earthquake, Japan. Ann Geofis 42:851–869

Yang W, Ben-Zion Y (2010) An algorithm for detecting clipped waveforms and suggested correction procedures. Seismol Res Lett 81:53–62

Yang X, Bondár I, Bhattacharyya J et al (2004) Validation of regional and teleseismic travel-time models by relocating ground-truth events. Bull Seism Soc Am 94:897–919

Zahradník J, Custódio S (2012) Moment tensor resolvability: application to southwest Iberia. Bull Seism Soc Am 102:1235–1254

Zaliapin I, Ben-Zion Y (2015) Artifacts of earthquake location errors and short-term incompleteness on seismicity clusters in southern California. Geophys J Int 202:1949–1968

Zitellini N, Gràcia E, Matias L et al (2009) The quest for the Africa–Eurasia plate boundary west of the Strait of Gibraltar. Earth Planet Sci Lett 280:13–50

Zotov OD (2007) Weekend effect in seismic activity. Izv Phys Solid Earth 43:1005–1011

Zúñiga FR, Wiemer S (1999) Seismicity patterns: are they always related to natural causes? Pure Appl Geophys 155:713–726